

ANALYSIS OF A CERAMIC RADOME

February 1979

19990518 042

Approved for Public Release;
Distribution Unlimited

**AEROSPACE STRUCTURES
INFORMATION AND ANALYSIS CENTER**


**OPERATED FOR THE AIRFORCE FLIGHT DYNAMICS LABORATORY
BY ANAMET LABORATORIES, INC.**

February 26, 1979

This report summarizes the analysis conducted to determine the thermal stresses in a ceramic radome subjected to laser irradiation. It describes the thermal analysis conducted to determine the thermal loading in laboratory test discs and in a full-size radome model based on a "Sparrow" radome. It also describes the structural analysis of both structures based on the thermal loading derived and compares these results to a one-dimensional thermal and thermal stress analysis. This work was performed under ASIAC Problem No. 105.

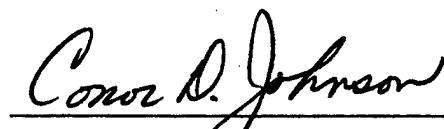
The work was done by the Aerospace Structures Information and Analysis Center, which is operated for the Air Force Flight Dynamics Laboratory by Anamet Laboratories, under Contract No. F33615-77-C-3046.

Submitted by:



Gordon R. Negaard
Principal Investigator

Approved by:



Conor D. Johnson, Ph.D.
Program Manager

TABLE OF CONTENTS

| <u>Section</u> | <u>Page No.</u> |
|------------------------------|-----------------|
| 1 INTRODUCTION | 1 |
| 2 THERMAL ANALYSIS | 6 |
| 3 DISC ANALYSIS | 11 |
| 4 RADOME ANALYSIS | 44 |
| 5 SUMMARY | 62 |
| REFERENCES | 64 |

SECTION 1 INTRODUCTION

This study was conducted for the Air Force Materials Laboratory to analytically determine the thermal stresses in a silicon nitride ceramic radome under laser irradiation.

Ceramic materials tested for use as laser hardened radomes on air-to-air missiles have been demonstrated to fail by thermal stress under such irradiation. One technique for evaluating these materials is to conduct tests using small scale disc specimens with a laboratory laser. The stress states obtained in such a test are different from those developed in a full-scale radome. This is partly due to the difference in heat flux between a laboratory laser and radiation postulated as a threat level. It is also partly due to the three-dimensional shape of the radome and the difference in constraints in comparing a radome to a disc.

The study can be discussed in three sections. A thermal analysis was conducted to determine the temperature distribution in the structural models as a function of time and applied heat flux. A structural analysis was conducted on disc models to determine the stress distribution using these calculated temperature profiles. Finally a structural analysis was conducted on a finite element model of a typical radome using a three-dimensional temperature distribution.

NASTRAN was selected as the computer code to be used for the finite element structural analysis of the radome and disc models (Ref. [1]*). It was decided not to use the NASTRAN thermal analysis capability because it was necessary to consider sublimation of the surface material and variable thermal properties. An available thermal analysis code "LTA" (Ref. [2]) was used for the thermal analysis instead. This code possesses

*Numbers in brackets indicate References at end of report.

an ablation capability, however, it is limited to the ablation of ten nodal points. A considerable effort was made to rewrite this section of the code to remove this limitation, but was never successful. Instead, a one-dimensional heat transfer and thermal stress code written by Donald Paul, AFFDL/FBE (Ref. [3]), was used to perform the heat balance at the surface, taking sublimation into account. The surface temperature, as calculated by the one-dimensional code, was input to LTA as a function of time. LTA was then used to calculate a three-dimensional temperature distribution. The temperature distribution at selected times from LTA was then input to the NASTRAN models to obtain the thermal stress distributions. Based on the results of the AFFDL 1-D study, 0.03 seconds was selected for the threat level irradiation and 0.10 seconds was selected for the laboratory level irradiation as the times which provided the sharpest thermal gradients and highest thermal stresses.

The disc models used in the analysis were based on the size of the laboratory samples. The radome model used was based on the "SPARROW" air-to-air missile. The disc models were 0.29 inches thick while the radome model was 0.26 inches thick. In both cases, this is less than the diameter of the beam so that the temperature distribution approximates a one-dimensional state except near the edge of the beam. The temperatures and stresses can thus be compared to those obtained from a one-dimensional analysis in the central part of the beam.

An LTA model consists of a mesh of capacitors and resistors connecting the capacitors. The capacitors represent the heat capacity of the material while the resistors model the thermal conduction. A preprocessor, THREM3D, was used to simplify the use of LTA. THREM3D accepts the mesh as input and generated most of the necessary data cards for LTA. Mesh generators were written for both the disc and the radome in order to simplify the input to THREM3D. A postprocessor was also written to convert the output of LTA to grid point temperature cards

suitable for input to NASTRAN. Figure 1 provides a flow chart which illustrates the progression of these steps and also serves to clarify the terminology used in comparing stresses and temperatures.

The silicon nitride material properties used in this analysis are given in Table 1. These values are all temperature dependent, and NASTRAN, LTA, and the AFFDL 1-D program used linear interpolation between the given values to determine the material and mechanical properties at each node at each time step. A temperature independent density of 0.09034 lb/in.^3 and a Poissons ratio of 0.25 were assumed.

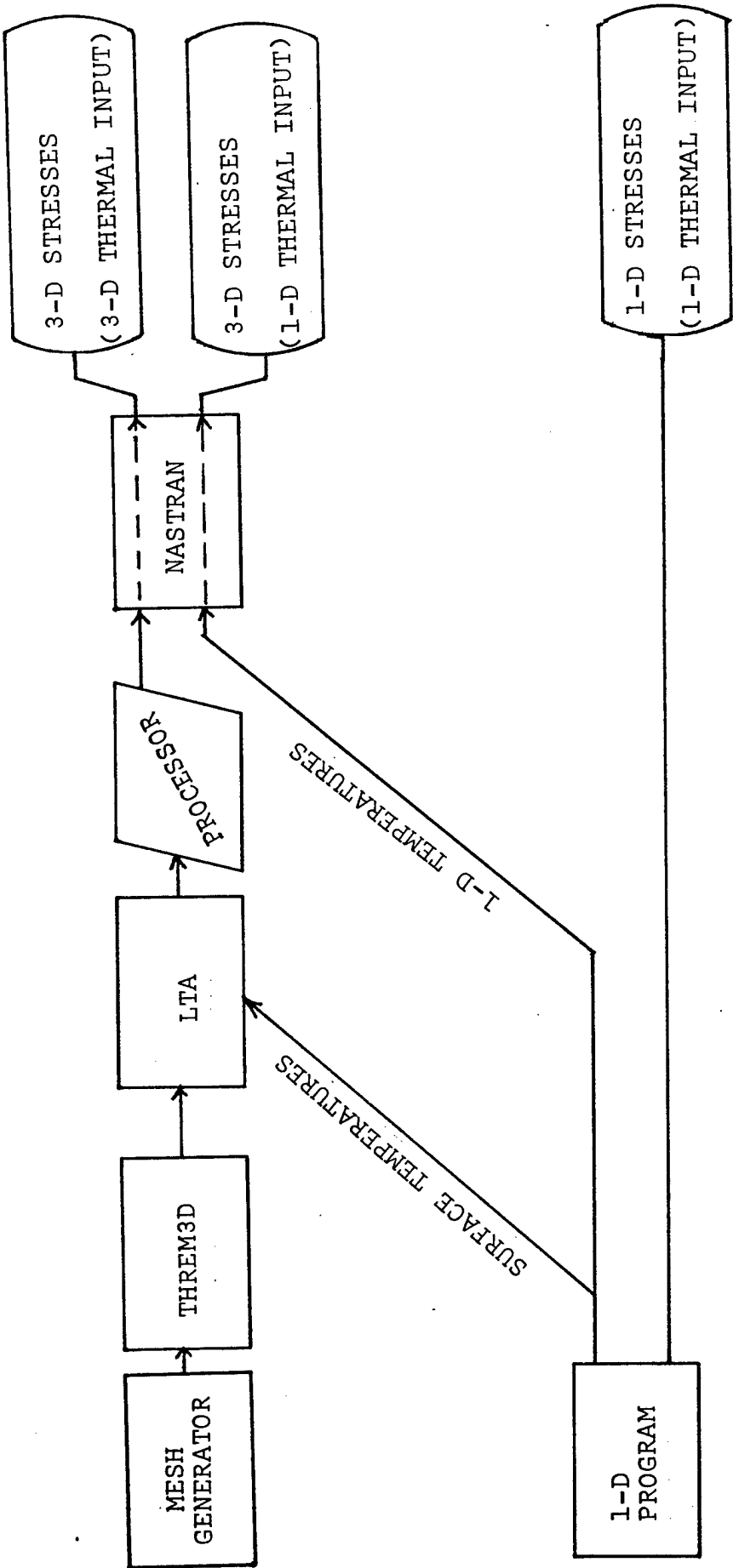


Figure 1. Analysis Flow Chart

TABLE 1
SILICON NITRIDE PROPERTIES

| TEMP. (°R) | YOUNG'S MODULUS (10 ⁶ psi) | COEFFICIENT OF LINEAR THERMAL EXPANSION (10 ⁻⁶ in/in/°R) | THERMAL CONDUCTIVITY (10 ⁻³ BTU/ft-sec-°R) | SPECIFIC HEAT (BTU/lb-°R) |
|---------------|--|---|--|------------------------------|
| 460 | - | - | 1.56 | .10 |
| 530 | 19.6 | 1.00 | - | - |
| 960 | - | - | - | .21 |
| 1160 | - | - | - | .24 |
| 1260 | - | - | 1.28 | - |
| 1360 | - | - | - | .26 |
| 1660 | - | 1.25 | - | - |
| 2060 | - | - | 1.11 | - |
| 2260 | - | 1.56 | - | - |
| 2860 | 16.6 | 2.00 | - | - |
| 3460 | 12.6 | 2.20 | .917 | .37 |
| 4060 | 8.6 | 2.20 | - | - |
| 4460 | 1.0 | 2.20 | - | - |
| 5460 | 1.0 | 2.20 | - | - |

SECTION 2

THERMAL ANALYSIS

The radiation characteristic of a laser pulse is of high intensity and short duration. It was assumed that thermal gradients would be high, creating thermal shock. The one-dimensional heat transfer and thermal stress analysis performed by Donald Paul, AFFDL/FBE, indicated this to be the case. Surface temperatures quickly rose to the point where sublimation of the surface material would begin. Although the NASTRAN program has a thermal analysis capability, it does not consider sublimation or variable thermal properties. It was decided to use the Lockheed Thermal Analyzer Code (LTA) because it contains an ablation capability and handles variable thermal properties.

The LTA ablation capability is limited to ten nodes. Attempts were made to increase this since many more ablation nodes were needed for the radome model. This was unsuccessful since ablation was tied to the use of other core memory. All of the efforts to rewrite the ablation subroutine led to overwriting of other sections of the code. In order to consider the heat balance at the surface, it was decided to use the AFFDL 1-D thermal analysis code to provide surface temperatures as a function of time for LTA. The 1-D code balanced the flux at the surface with sublimation and heat conduction into the silicon nitride. Stresses were calculated through a numerical integration technique and temperatures through a finite difference method. The grid used was very fine containing 70 elements through the thickness with a spacing of 0.002 inches in the high thermal gradient region. Time steps were varied to insure excellent convergence. These surface temperatures were then used as input for LTA, and a 3-D temperature distribution was calculated based solely on thermal conduction. The assumption was made that the temperature and stress distributions obtained from the 1-D analysis were essentially correct

and that the temperature distribution obtained from LTA and the stress distribution obtained from NASTRAN could be compared to the 1-D results.

LTA was originally written as a two-dimensional code using a R-C circuit analogue, but has been modified to provide a three-dimensional thermal distribution. A three-dimensional problem, however, quickly runs into difficulties because of limitations on problem size. In theory, LTA can have as many as 4000 nodes. In practice, however, this number is limited by the formula

$$\sum_{i=1}^{NC} R_i + N_C \leq 5000.$$

In this formulation, NC is the number of nodal points and R_i is the number of connections leading from node i to the adjacent nodes. In a two-dimensional rectangular array, R_i will be four in the interior and three along an edge so that LTA could originally handle 1000 nodes or more. In a three-dimensional structure, however, R will be six in the interior, five on a surface, and four on an edge. If all the nodes are interior points, this corresponds to a limit of 714 nodes.

An axisymmetric formulation was used for the NASTRAN model of the disc requiring only a two-dimensional model, but it was necessary to model a pie-shaped wedge in order to use the three-dimensional LTA program and model the effect of the increased volume for heat conduction as the radius increases. A five degree wedge was chosen in order to keep the aspect ratios close to one in the heated region. This model contained 768 nodes, 384 on each face. Since these were all surface nodes, this model was within the LTA limitations without any major rewrite of the program. It was necessary, however, to increase the internal storage from the original 15,000 to 25,000 to accomplish this. This LTA model required 2000 CP seconds and 144,400 words of central memory to run on a CDC 6600. It was limited not by the computer, but by the internal storage algorithms. It was sufficient to handle the disc model since it was not necessary to model the entire disc, only the part of the disc

affected by the temperature distribution. In Figure 2, this corresponds to the shaded area. The structural model for NASTRAN included the entire disc, but because the disc was modeled using axisymmetric elements, requiring essentially only a 2-D characterization, this was well within practical computer limits. The contour plots shown later are also limited to this shaded area.

The radome thermal analysis was based on the experience gained from using LTA on the disc and upon the results of a free plate study (Ref. [4]) using solid isoparametric elements. It was necessary to model one-half the shell-of-revolution for the NASTRAN analysis, but this region was narrowed to include only the region affected by the heating for LTA. This corresponds to the area shown in the contour plots of the radome. A compromise had to be made between the number of nodal points through the thickness and the density of the mesh for both NASTRAN and LTA. With judicious juggling of the internal storage locations and by increasing the total storage as much as possible, the LTA radome model was increased to 1078 nodal points. This required 174,000 octal words of central memory and approximately 1000 CP seconds to run. This larger model still ran twice as fast as the disc model, because of the size of the time step used. LTA automatically chooses a time step compatible with the smallest internal dimension. Since the mesh in the disc was very fine compared to the radome, this time step was approximately 3.3 microseconds for the disc compared to 12.4 microseconds for the radome. The upper limit on nodal points was not based on computer limitations, but on the storage algorithm within LTA. Increasing the storage dimensions beyond 33,000 words resulted in numbers too large for storage. Therefore, the structural analysis of the radome was limited by LTA rather than by NASTRAN although the NASTRAN model was about as large as was economically feasible.

An alternate approach to using LTA to generate the NASTRAN grid point temperatures was investigated. A one-dimensional

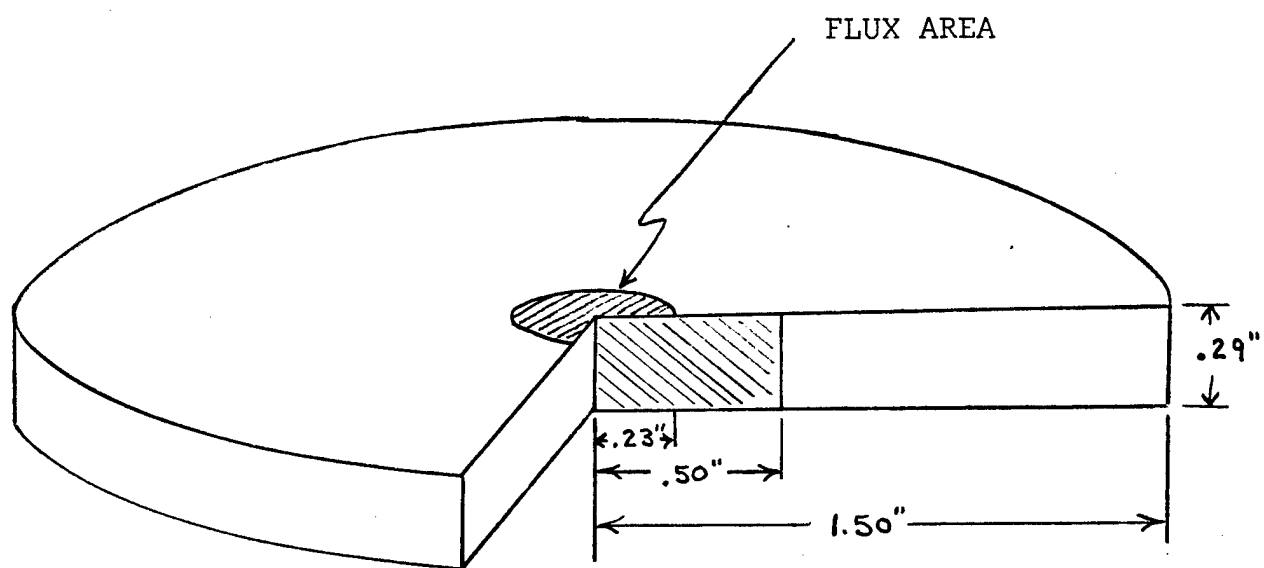


Figure 2. Ceramic Disc Model

temperature profile through the thickness was input for each surface node in the structural model. These profiles were obtained from the AFFDL 1-D thermal program adjusted for the flux level at the surface position. This approach allowed one to get around the limitation of LTA and only be bound by the limitations on NASTRAN. The results of this effort were ambiguous due to the mesh spacing, but appears to offer a possible alternative.

SECTION 3 DISC ANALYSIS

A model of the actual disc used as a laboratory test specimen was analyzed with a threat level heat flux. This provided information concerning the depth of peak stresses for use in modeling the radome. A heat flux representation of the laboratory laser was also used to obtain thermal stresses for comparison against laboratory behavior.

A NASTRAN axisymmetric element, CTRAPRG, was chosen for the analysis. Using this element, it was necessary to model only a radial cross-section of the disc from the center to the edge of the disc as shown in Figure 2. A uniform grid spacing through the thickness was used for the original NASTRAN disc model illustrated as DISC 1 in Figure 3. The spacing used for the LTA model is shown in Figure 4. The LTA temperature distributions and the NASTRAN stresses were compared to the one-dimensional results. Two iterations of these models were made to ensure that NASTRAN was obtaining the peak stresses. Examination of Figures 5 and 6 shows that the spacing for DISC 3 appears to be fine enough to pick up the maximum hoop stress obtainable. This was approximately 105,000 psi. compression at a depth of 0.0075 inches. The maximum tensile stress was approximately 11,000 psi. at a depth of 0.085 inches. The stress reverts to compression again on the bottom edge of the disc. By comparison, the one-dimensional analysis predicted 89,000 psi. compression at a depth of 0.0050 inches, and 14,300 psi. tension at a depth of 0.045 inches. The 1-D analysis predicted a stress reversal with a stress of 11,300 psi. compression at the heated surface. The DISC 3 mesh is fine enough to pick up this stress reversal, obtaining a surface stress of 13,800 psi. compression. The 1-D analysis is based on a free plate so that the radial and hoop stresses are identical. The axial stress (normal to the plate) is predicted to be zero. The NASTRAN analysis gave hoop and radial

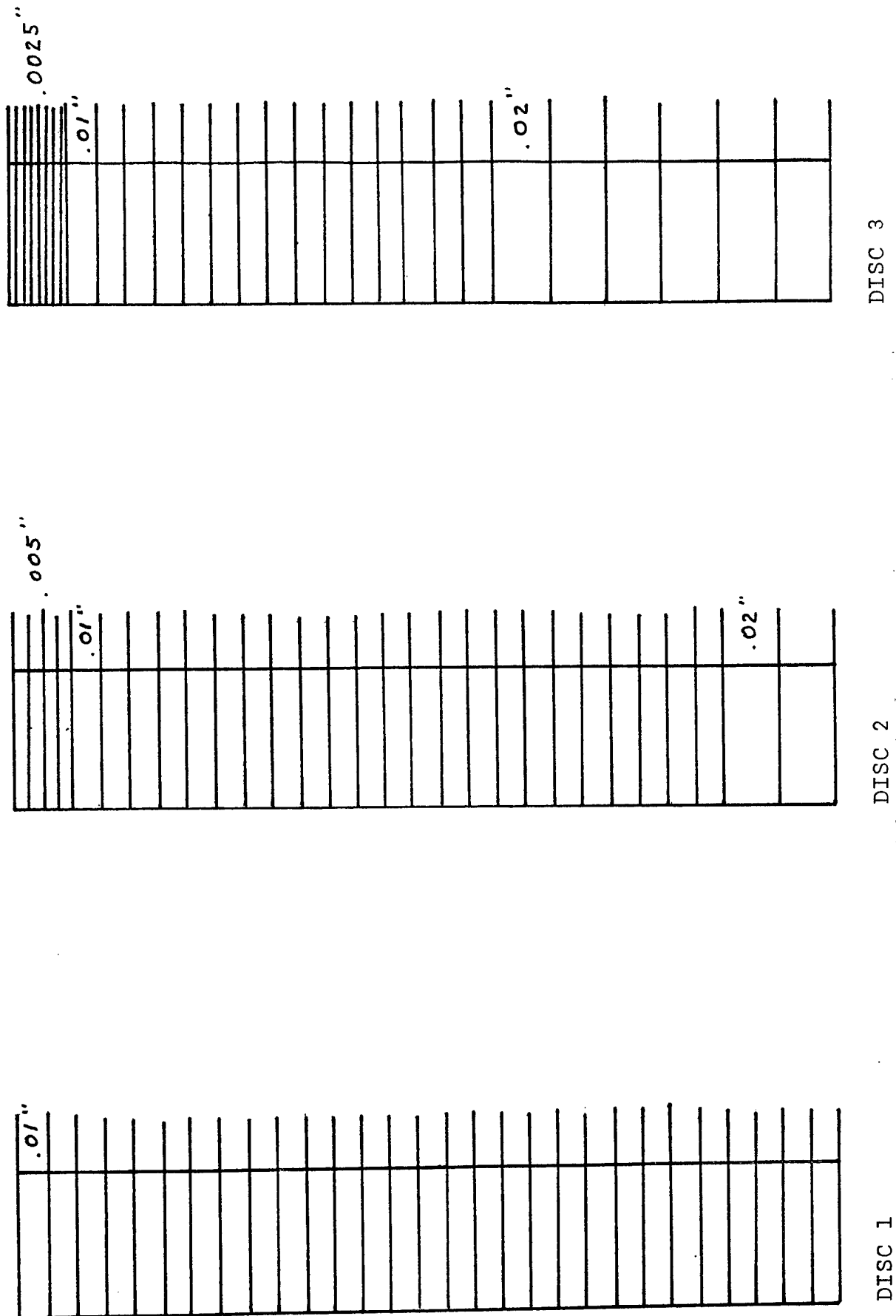


Figure 3. Grid Spacing for Structural Analysis

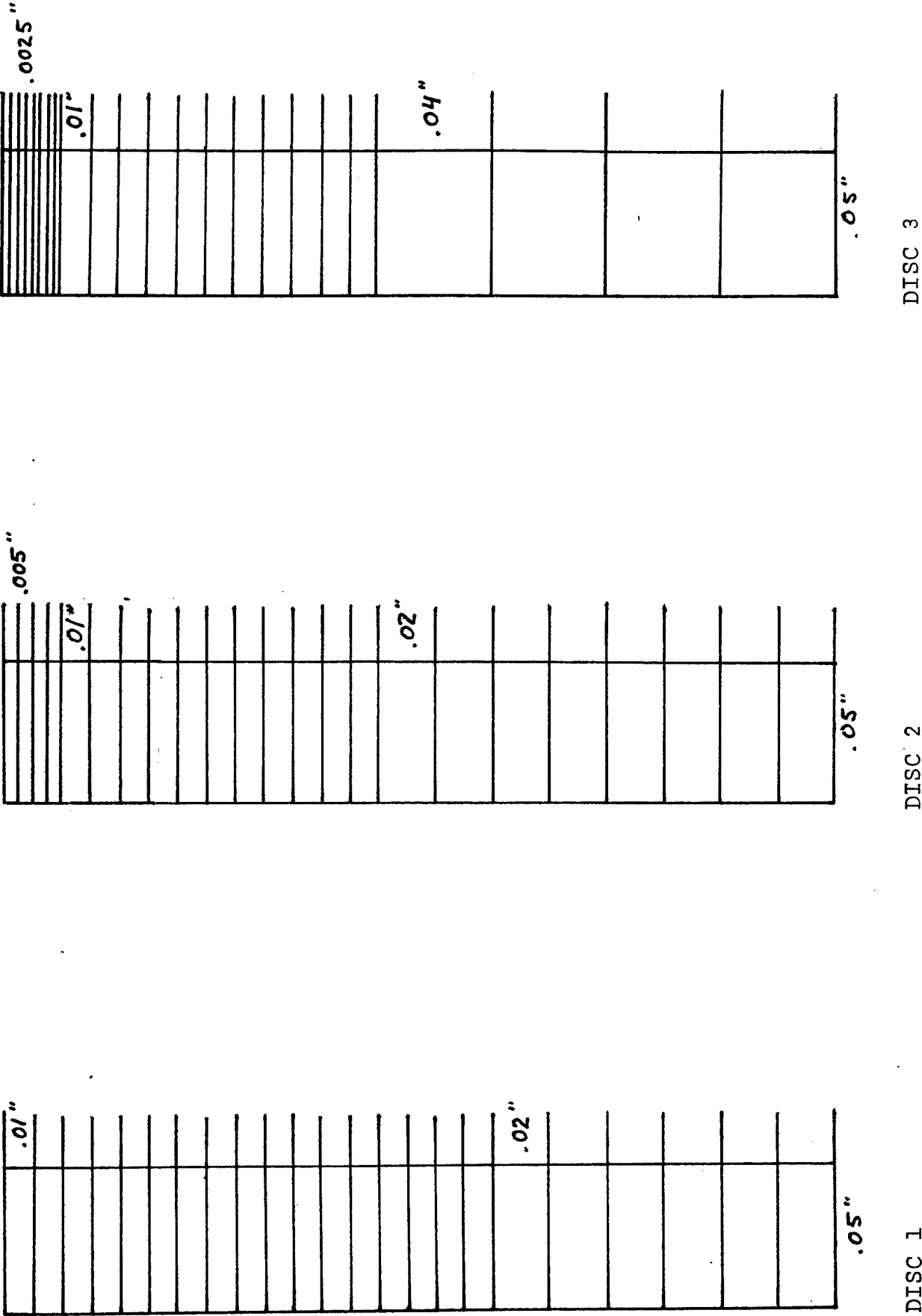


Figure 4. Grid Spacing for Thermal Analysis

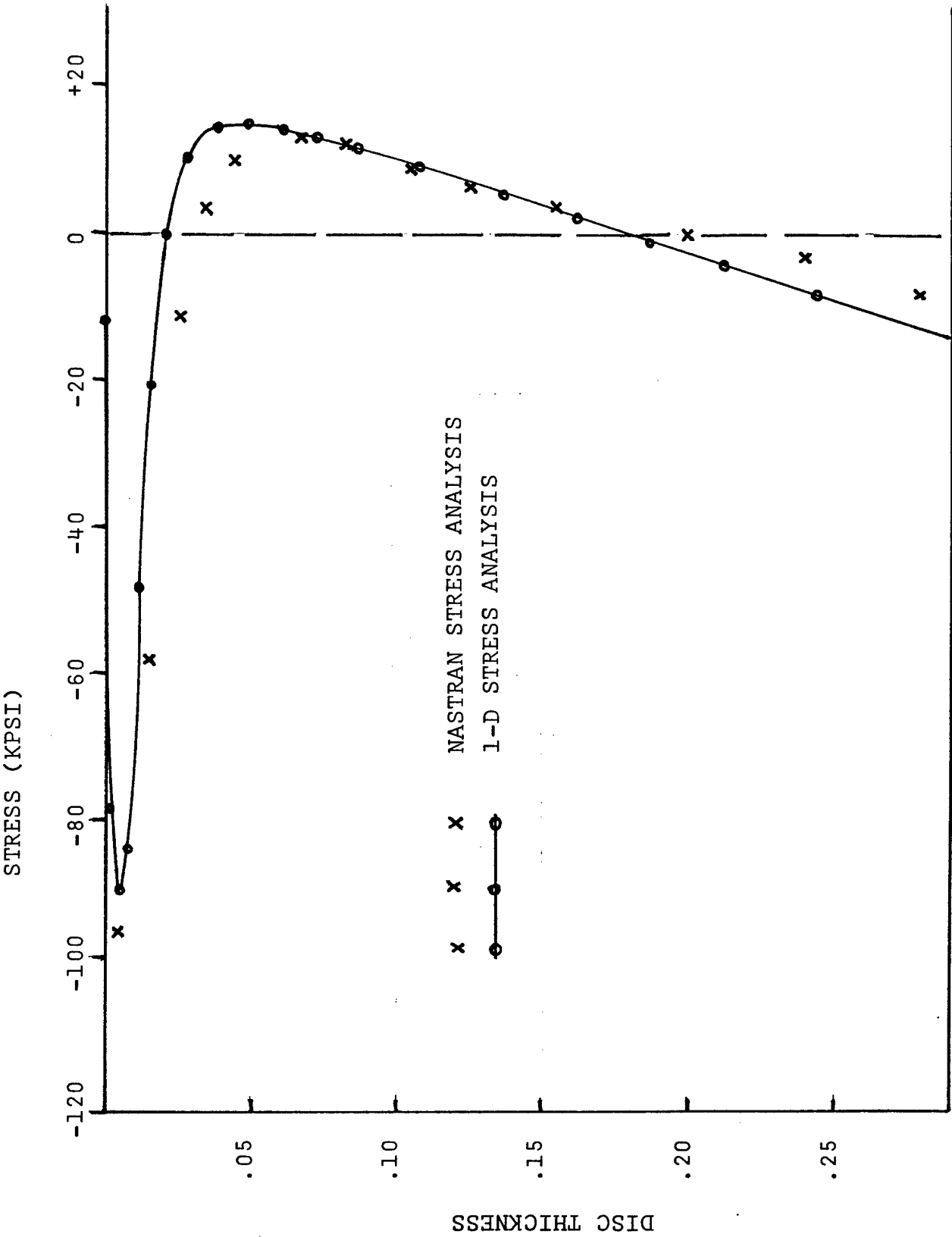


Figure 5. Hoop Stresses at Center of DISC 1 at 0.03 sec.

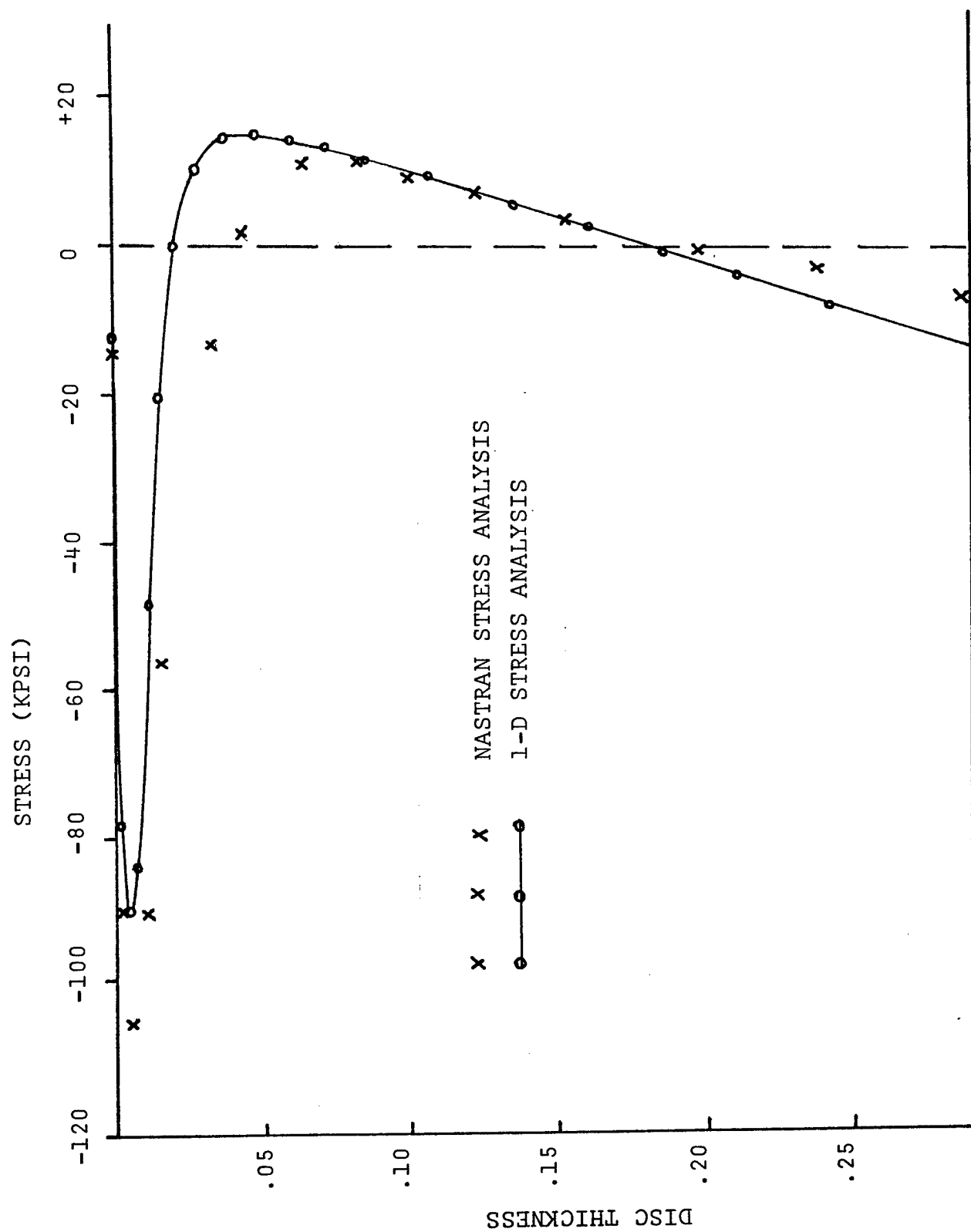


Figure 6. Hoop Stresses at Center of DISC 3 at 0.03 sec.

stresses that were nearly identical at the center of the beam, but diverged some away from the center.

A comparison of the LTA thermal prediction with the AFFDL 1-D results at 0.03 seconds is shown in Figure 7. It is apparent from this plot that LTA was not particularly sensitive to the geometry and that increasing the fineness of the mesh did not have much effect. It does not appear that it would approach the one-dimensional model in the limit. This difference can be explained in the difference in codes. The one-dimensional model takes additional second order effects into account, including ablation, while LTA results only included thermal conduction. For consistency in comparing the NASTRAN results, the temperature profile obtained from the LTA DISC 3 run was used for all three NASTRAN runs.

For additional comparisons, contour plots of axial, hoop, radial, and shear stresses for DISC 1 and DISC 3 were generated and are included as Figures 8 through 15. These were generated with the aid of a contour plotter and the reader must be cautioned in their interpretation. The plotter deletes contours that are too close together. They do serve, however, to show the shape of the areas of high stresses. For these plots, the left edge of the plot is the center of the disc. The portion shown represents only one-third of the cross-section, corresponding to the shaded area in Figure 2. The area of the disc subjected to heat flux is marked. The flux simulated in the analysis represents a flat beam. The surface temperatures input to LTA were identical everywhere within the beam although this would not be exactly true, even for the flat beam being simulated. The thermal distributions used for the results are shown in Figures 16 and 17. They are essentially one-dimensional except near the beam edge. The slight drop in temperature at the very center of the beam is due to the LTA program. Apparently the five-degree wedge used as a model created a slight anomaly at the point of the wedge since the three-dimensional effect is almost lost. In addition, LTA heat

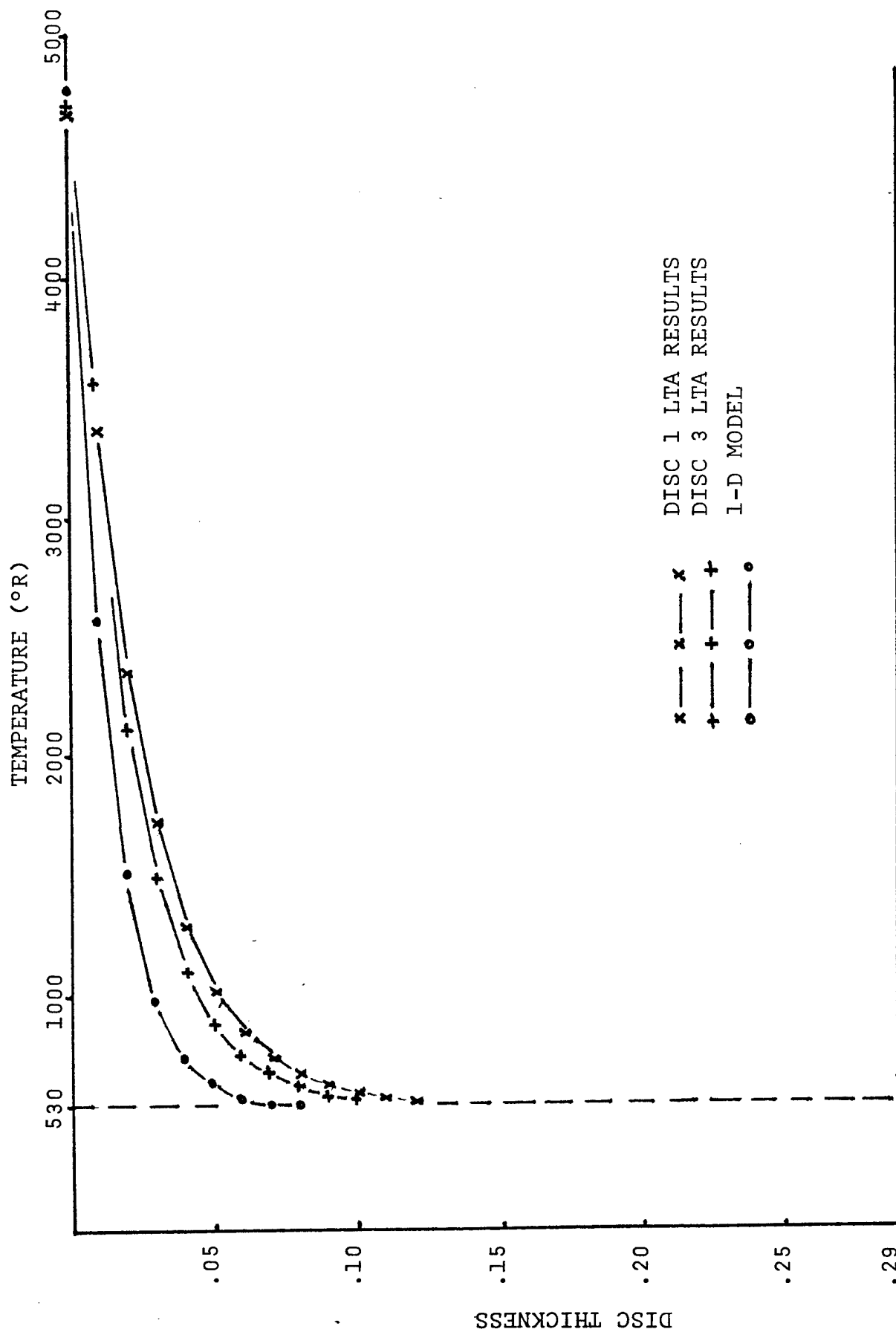


Figure 7. Temperature Gradients at Center of Disc at 0.03 sec.

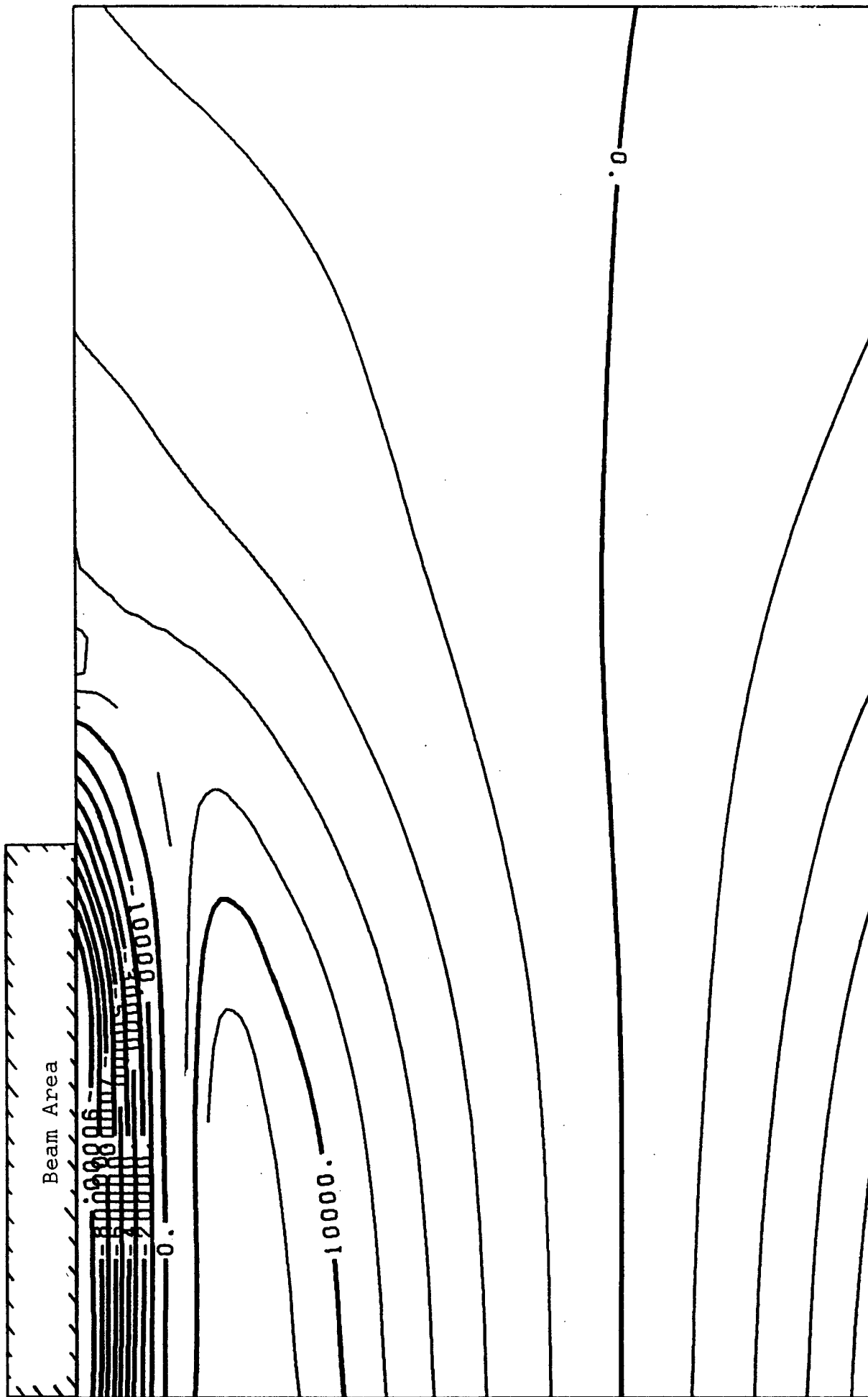


Figure 8. Hoop Stress Distribution, DISC 1, 0.03 sec.



Figure 9. Hoop Stress Distribution, DISC 3, 0.03 sec.

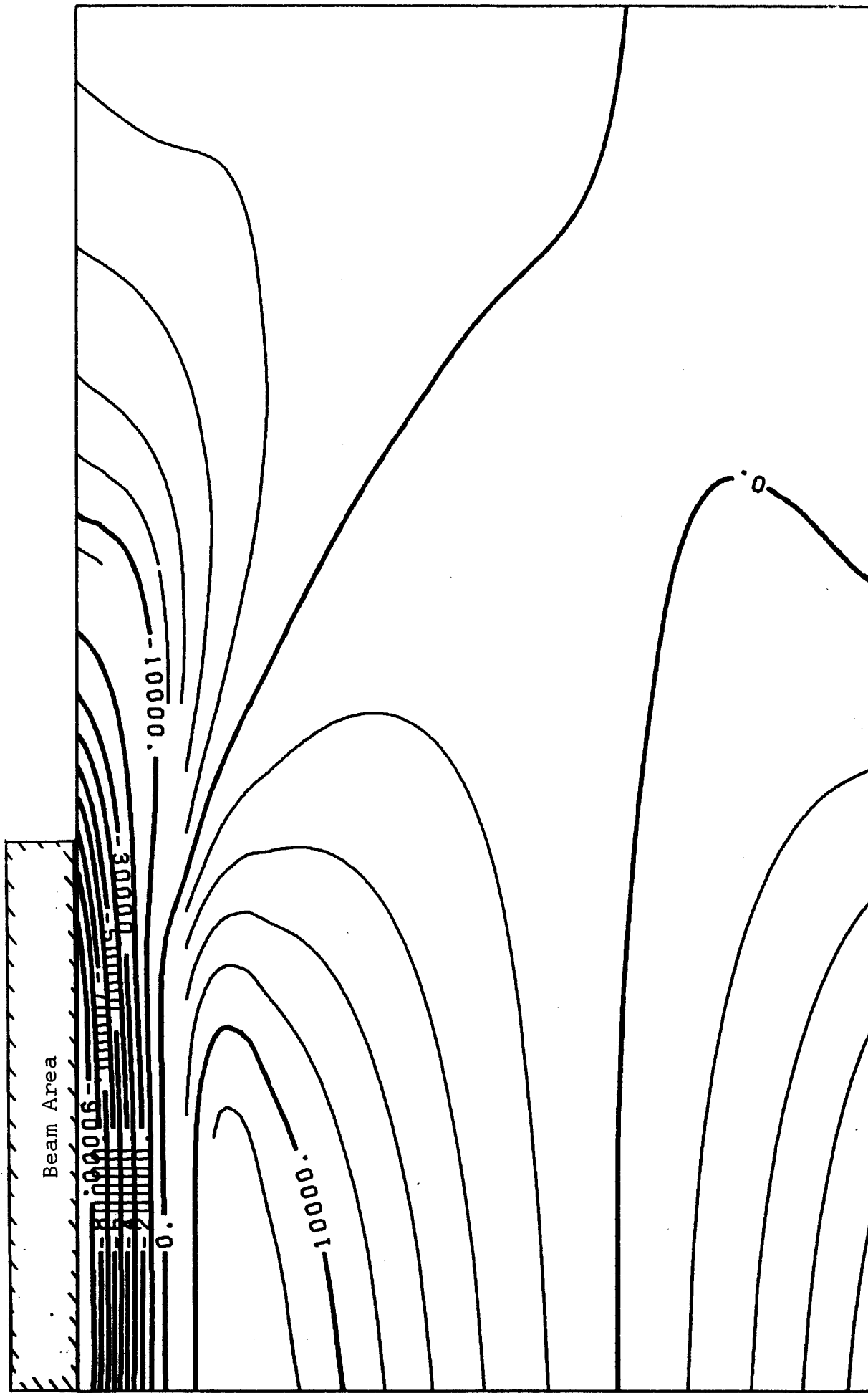


Figure 10. Radial Stress Distribution, DISC 1, 0.03 sec.

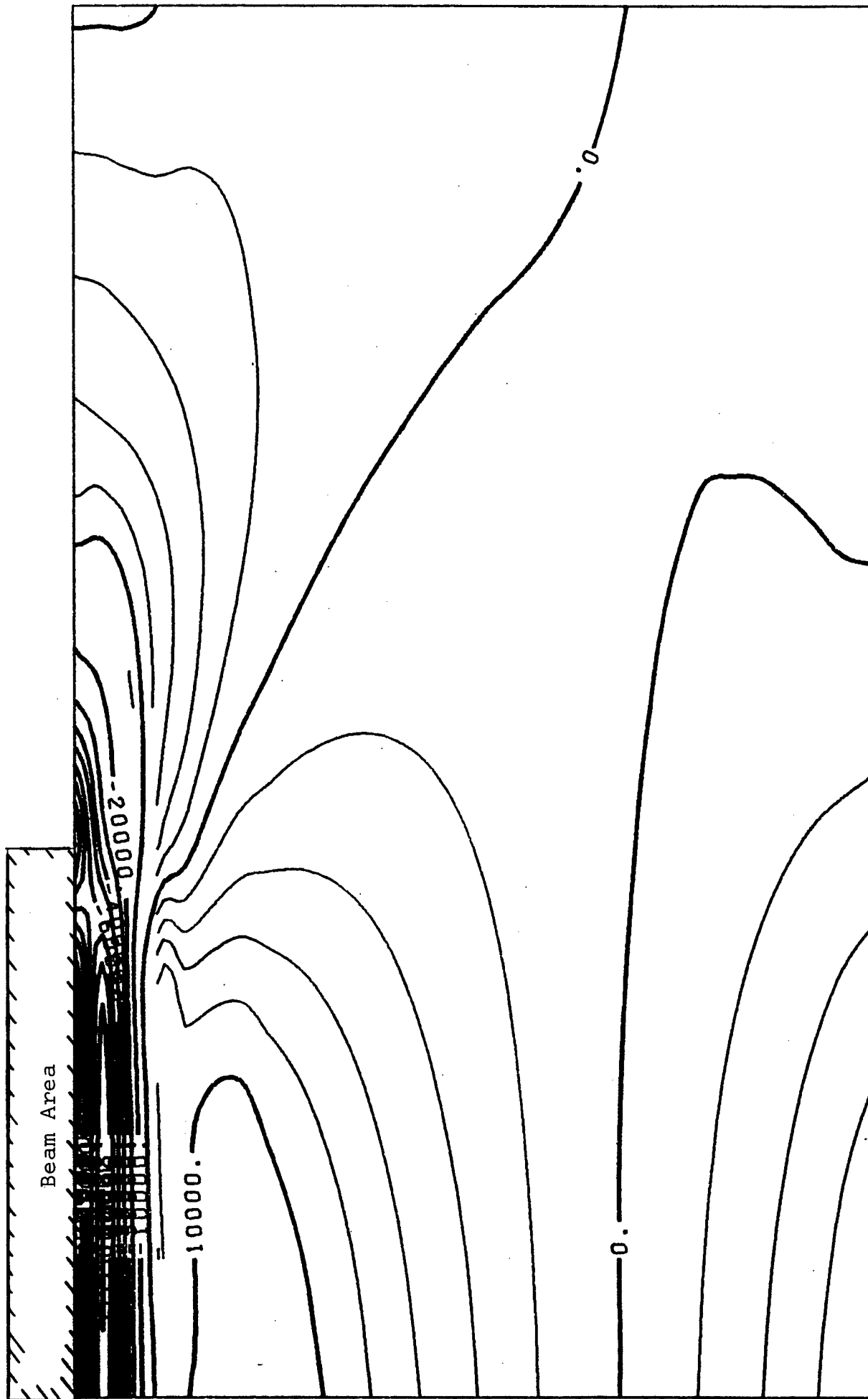


Figure 11. Radial Stress Distribution, DISC 3, 0.03 sec.

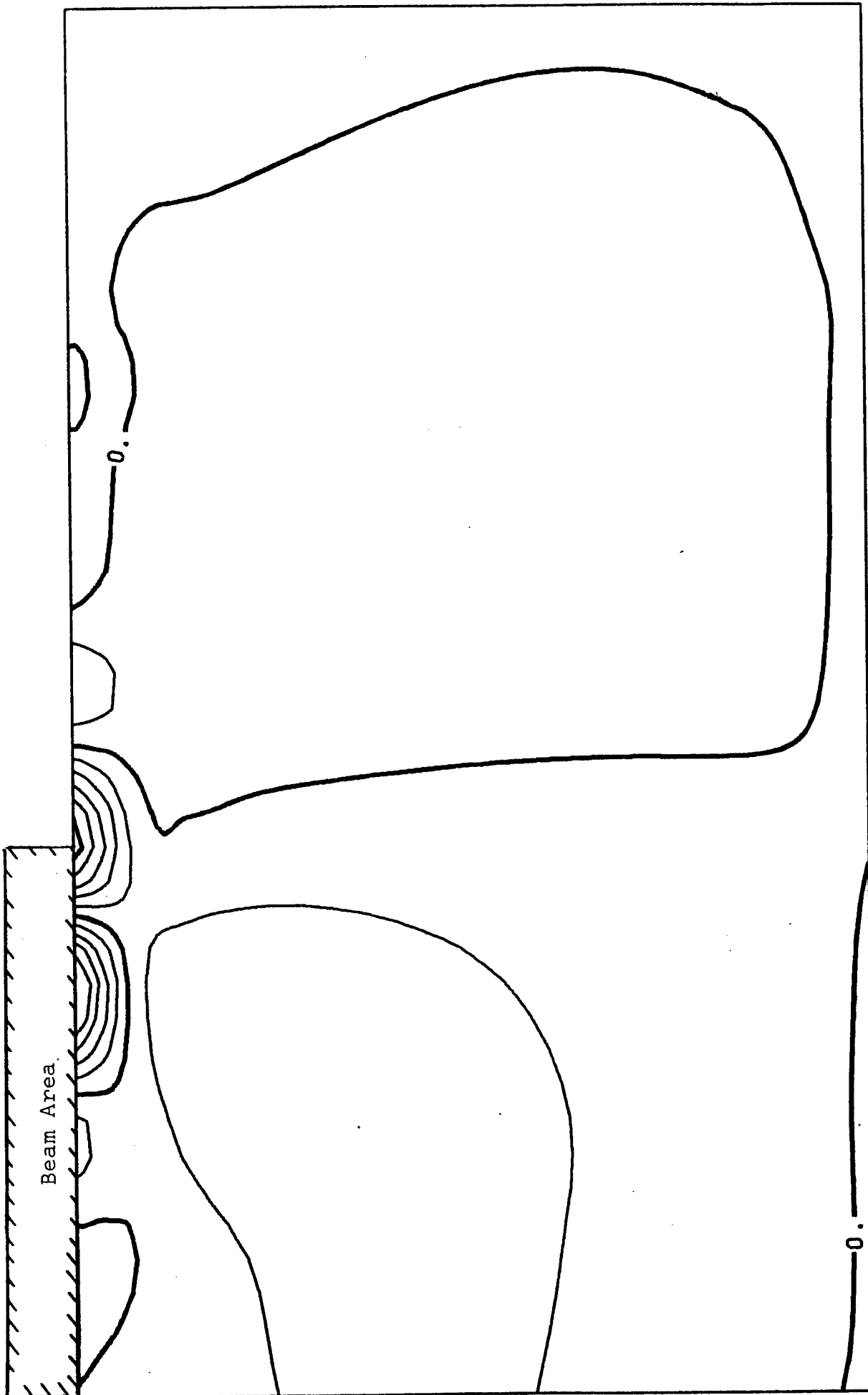


Figure 12. Axial Stress Distribution, DISC 1, 0.03 sec.

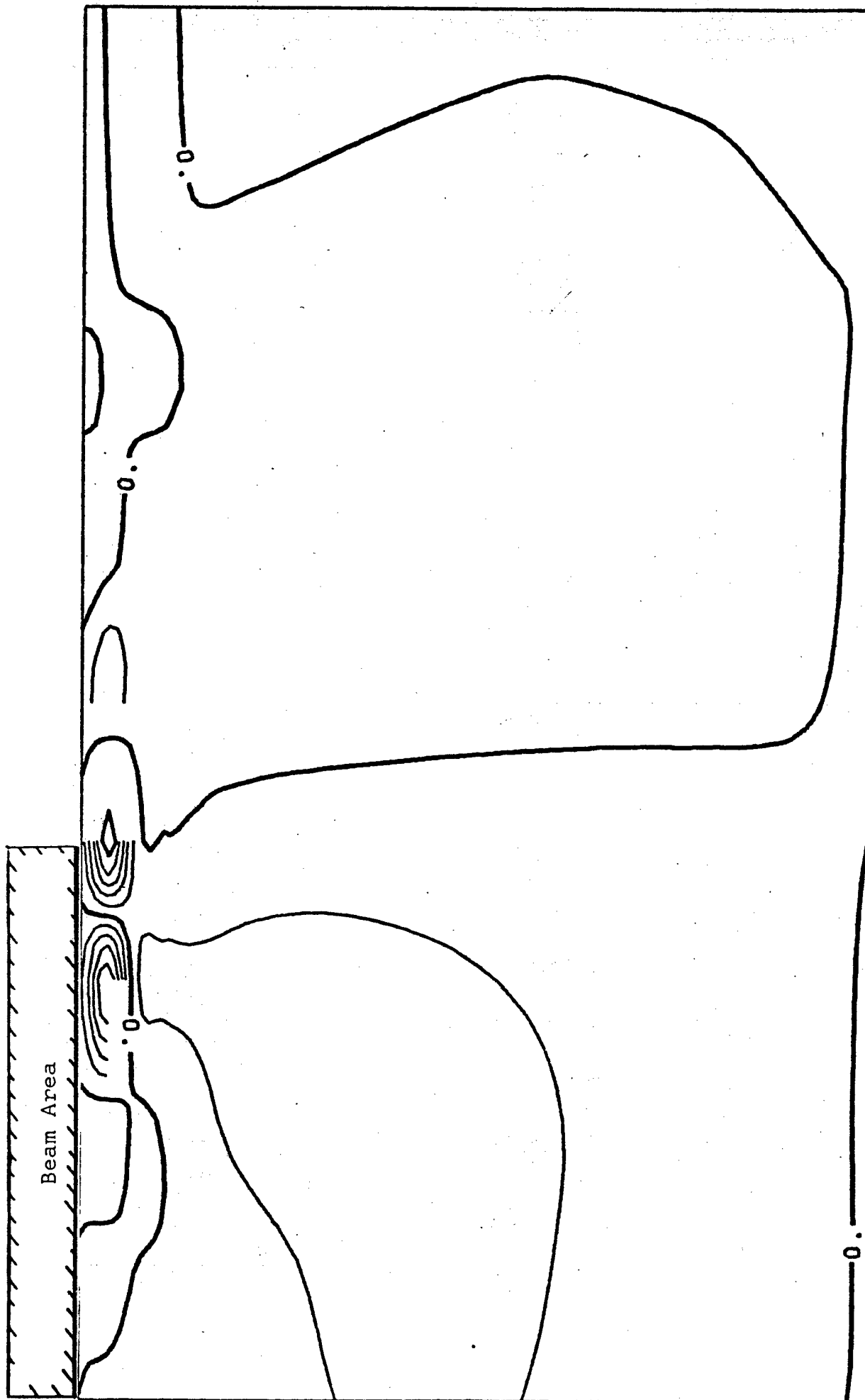


Figure 13. Axial Stress Distribution, DISC 3, 0.03 sec.

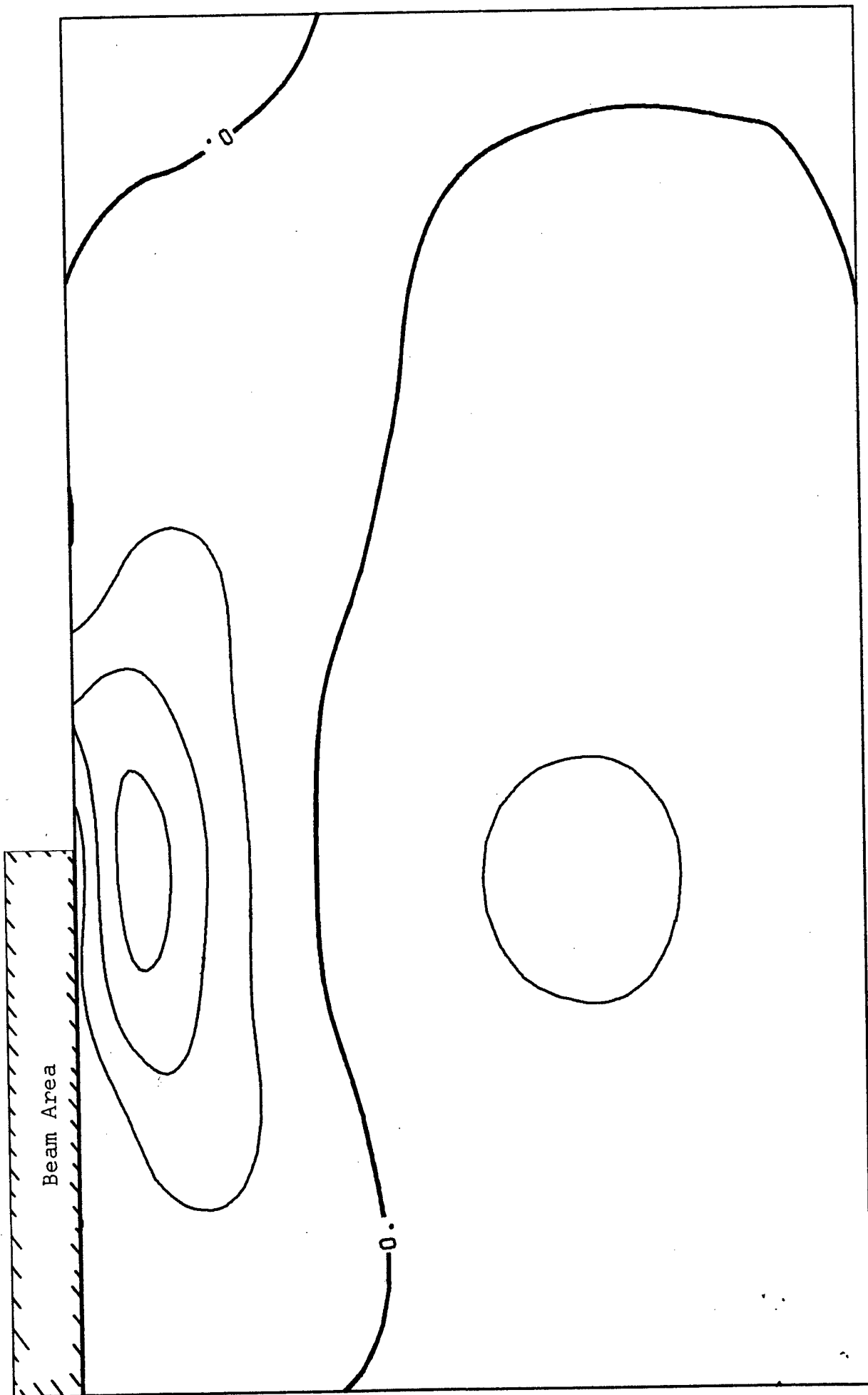


Figure 14. Shear Stress Distribution, DISC 1, 0.03 sec.

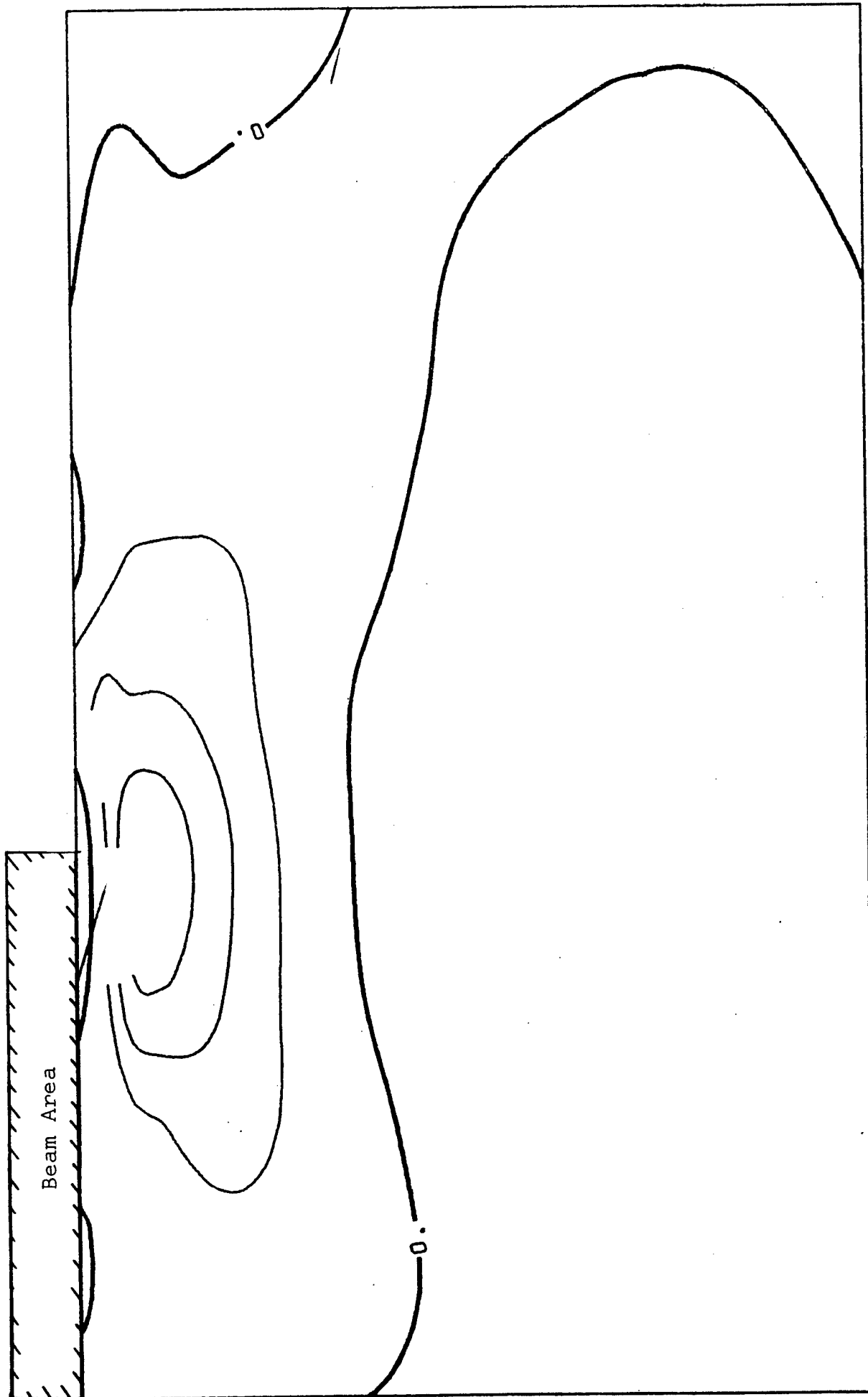


Figure 15. Shear Stress Distribution, DISC 3, 0.03 sec.

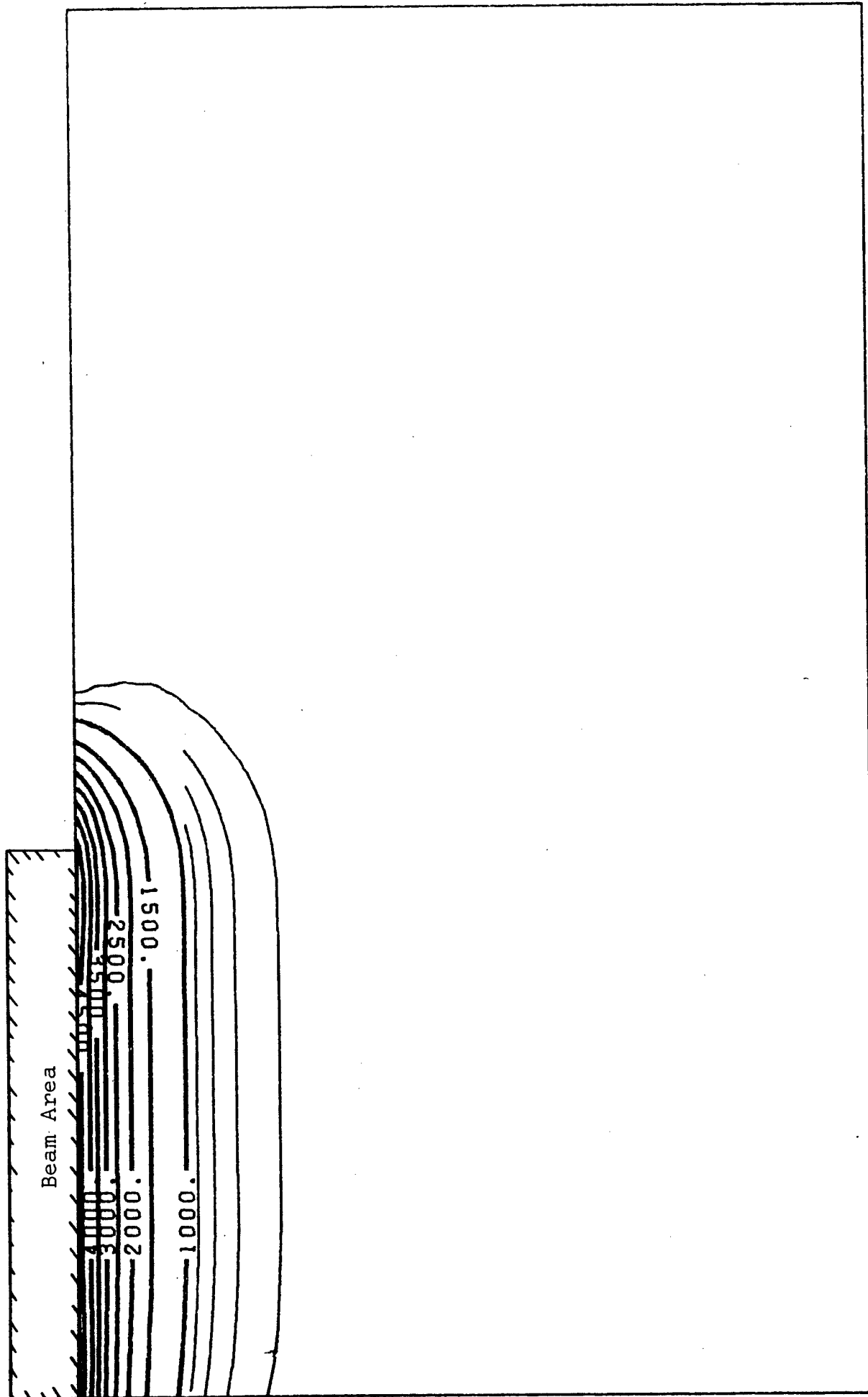


Figure 16. Temperature Distribution, DISC.1, 0.03 sec.

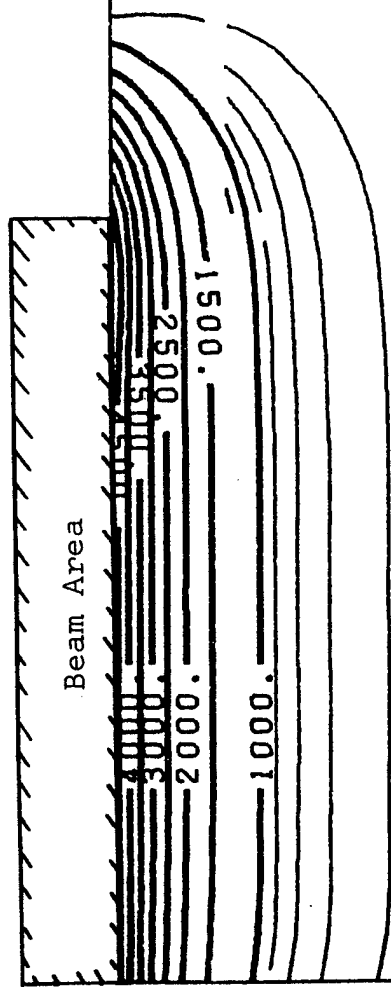


Figure 17. Temperature Distribution, DISC 3, 0.03 sec.

conduction along an edge was not as accurate as in the interior. From Figures 8 through 11, this does not appear to affect the radial or hoop stress prediction. These results showed that the mesh needed to be very fine in the radial direction near the outer surface of the radome. The shear and axial stresses are very small, as shown in Figures 12 through 15.

The same procedure was used to analyze DISC 3 subjected to the laboratory laser. The one-dimensional analysis showed peak stresses occurring at about 0.1 second compared to 0.03 seconds for the previous analysis. Contour plots of these temperature distributions are shown as Figures 18 through 27. Comparison of Figure 27 with Figure 17 shows a temperature gradient which extends further into the disc, but which has a shallower gradient than for the higher flux level. Plots of the stress distribution are shown as Figures 28 through 31. Hoop and radial stresses are essentially equal near the center of the disc, but they vary more at the edge of the beam than for the higher flux level used in DISC 3. This is apparently due to the fact that the peak stresses occur further below the surface than for the previous case. These peak stresses are about the same as for the higher flux of the threat level laser, approximately 12,000 psi. tensile and 90,000 psi. compressive, which is within the normal range of strength of silicon nitride materials.

Examination of the contour plots shows that the 1-D state of stress is essentially true at the center of the beam. It can be seen that the radial and hoop stresses are almost identical and that the axial and shear stresses are nearly zero. Peak compressive and tensile stresses can also be seen to occur at the center. From these contour plots and from Figures 5 and 6, it would appear that the 1-D analysis is reasonably accurate for a flat specimen under this type of thermal loading. It must be cautioned here that the thermal load was assumed to be constant across the surface of the beam as the input to LTA, however, the depth of the penetration of the heat flux can be

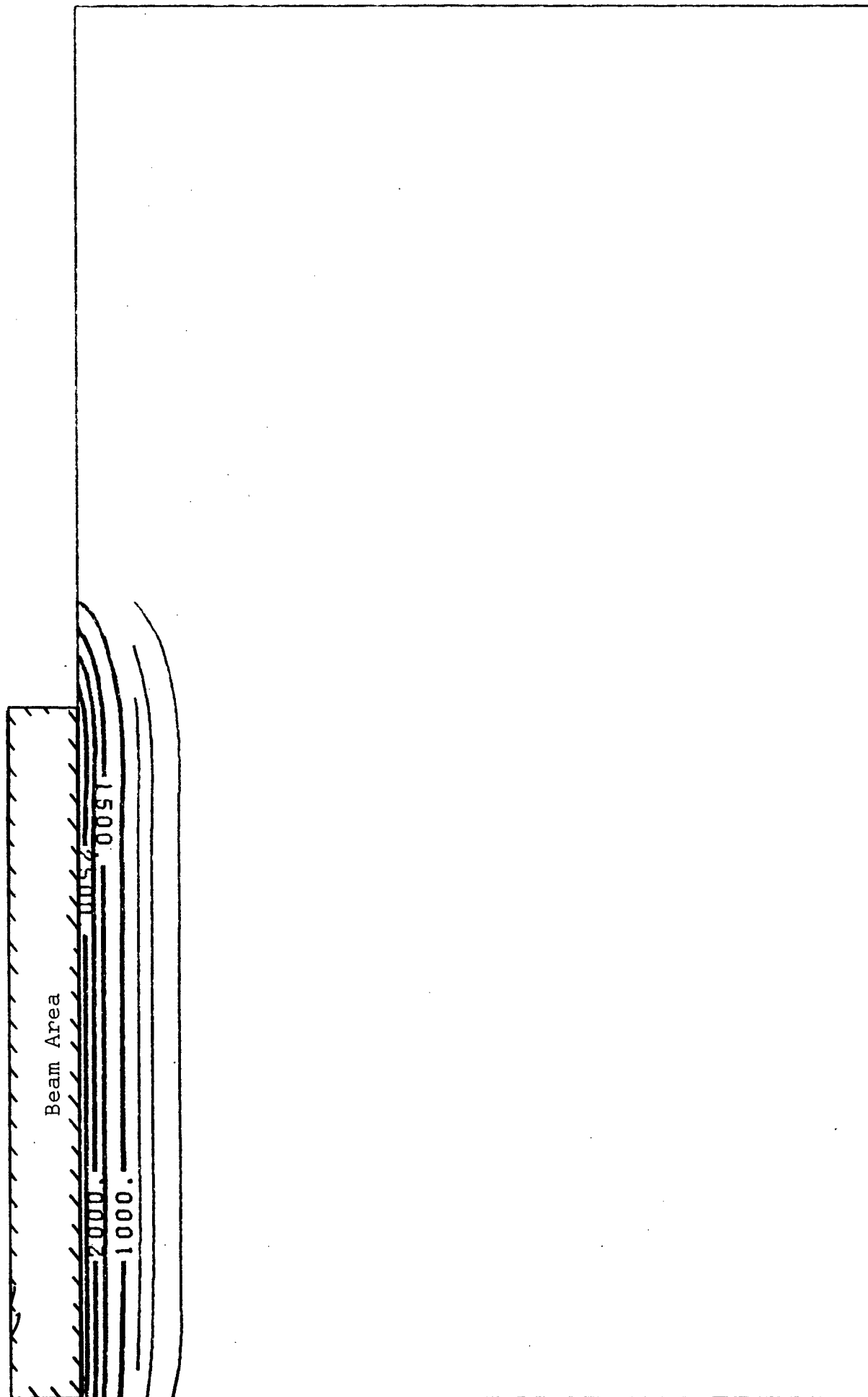


Figure 18. Temperature Distribution, DISC 3C, 0.01 sec.

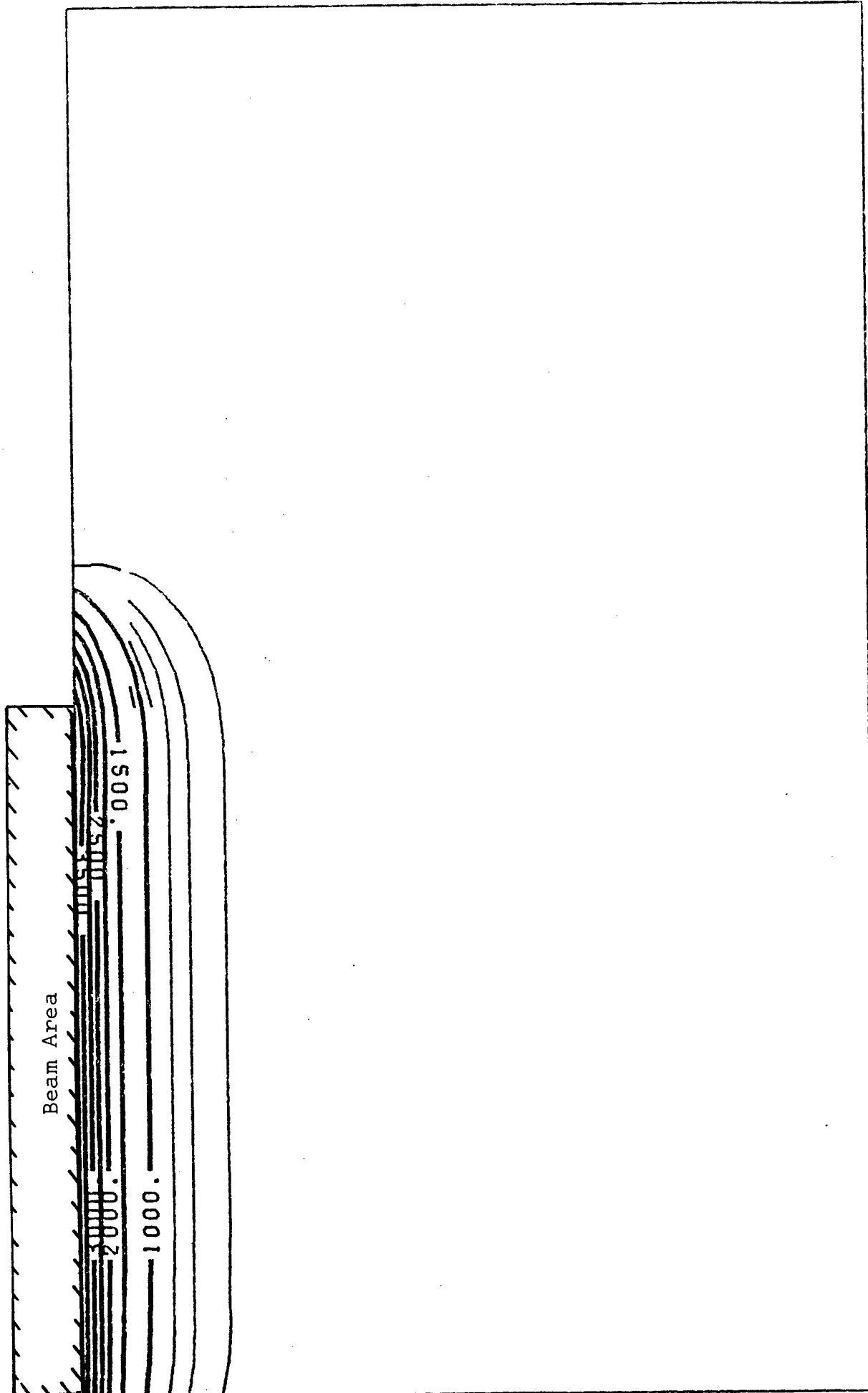


Figure 19. Temperature Distribution, DISC 3C, 0.02 sec.

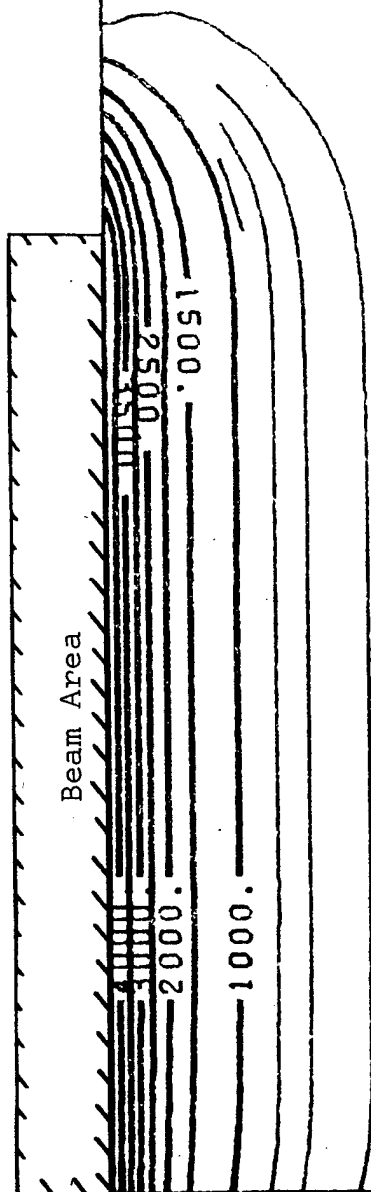


Figure 20. Temperature Distribution, DISC 3C, 0.03 sec.

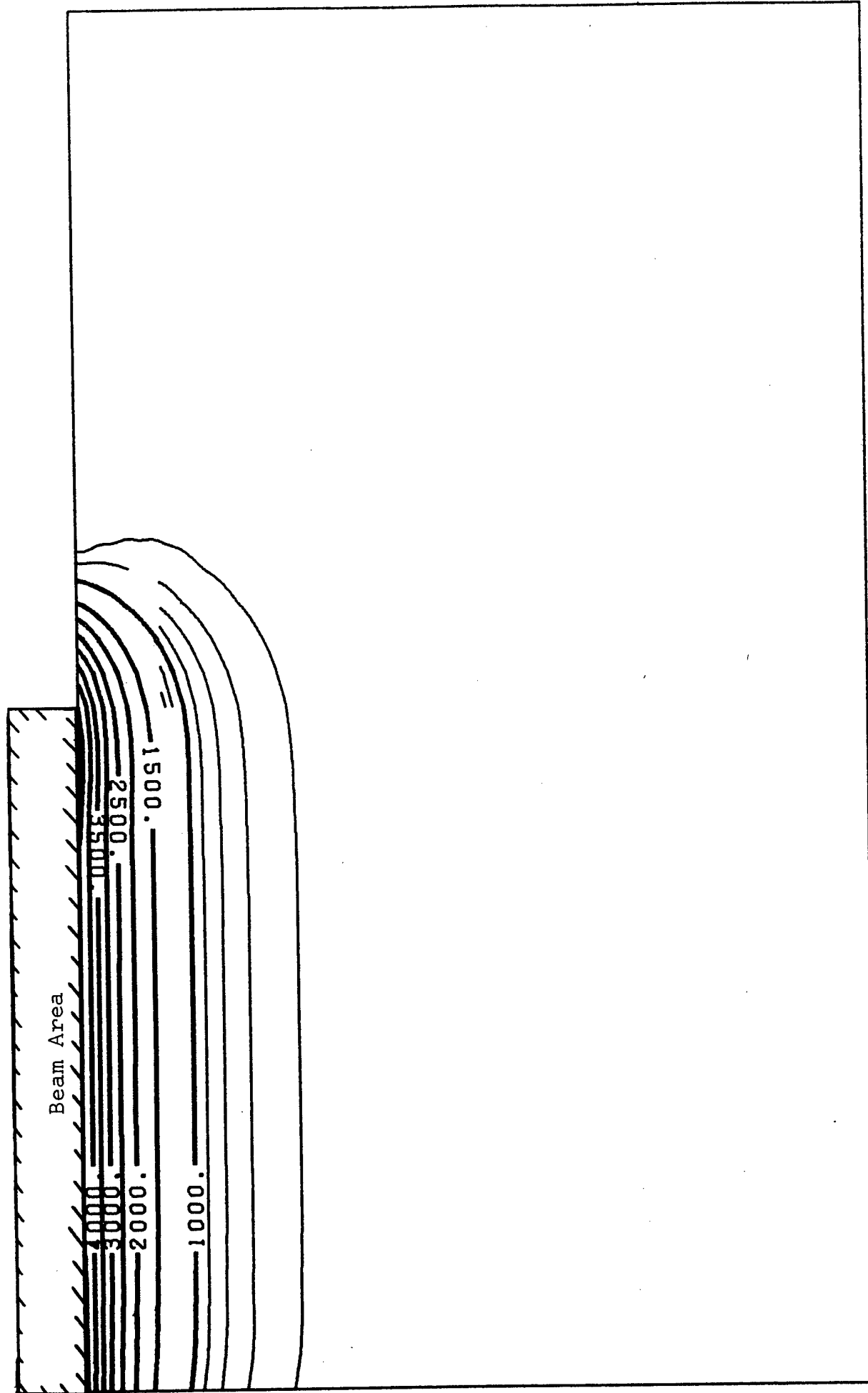


Figure 21. Temperature Distribution, DISC 3C, 0.04 sec.

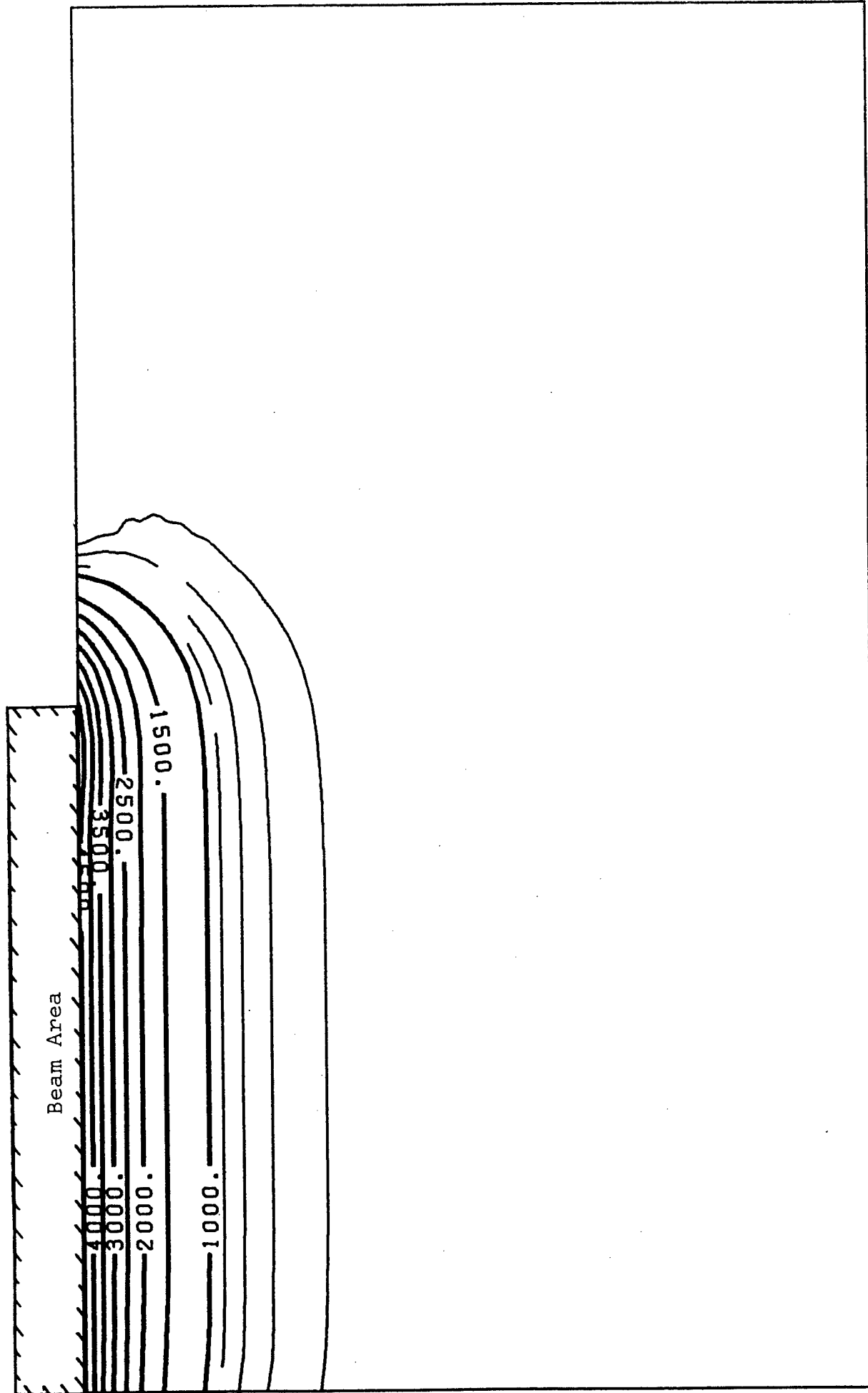


Figure 22. Temperature Distribution, DISC 3C, 0.05 sec.

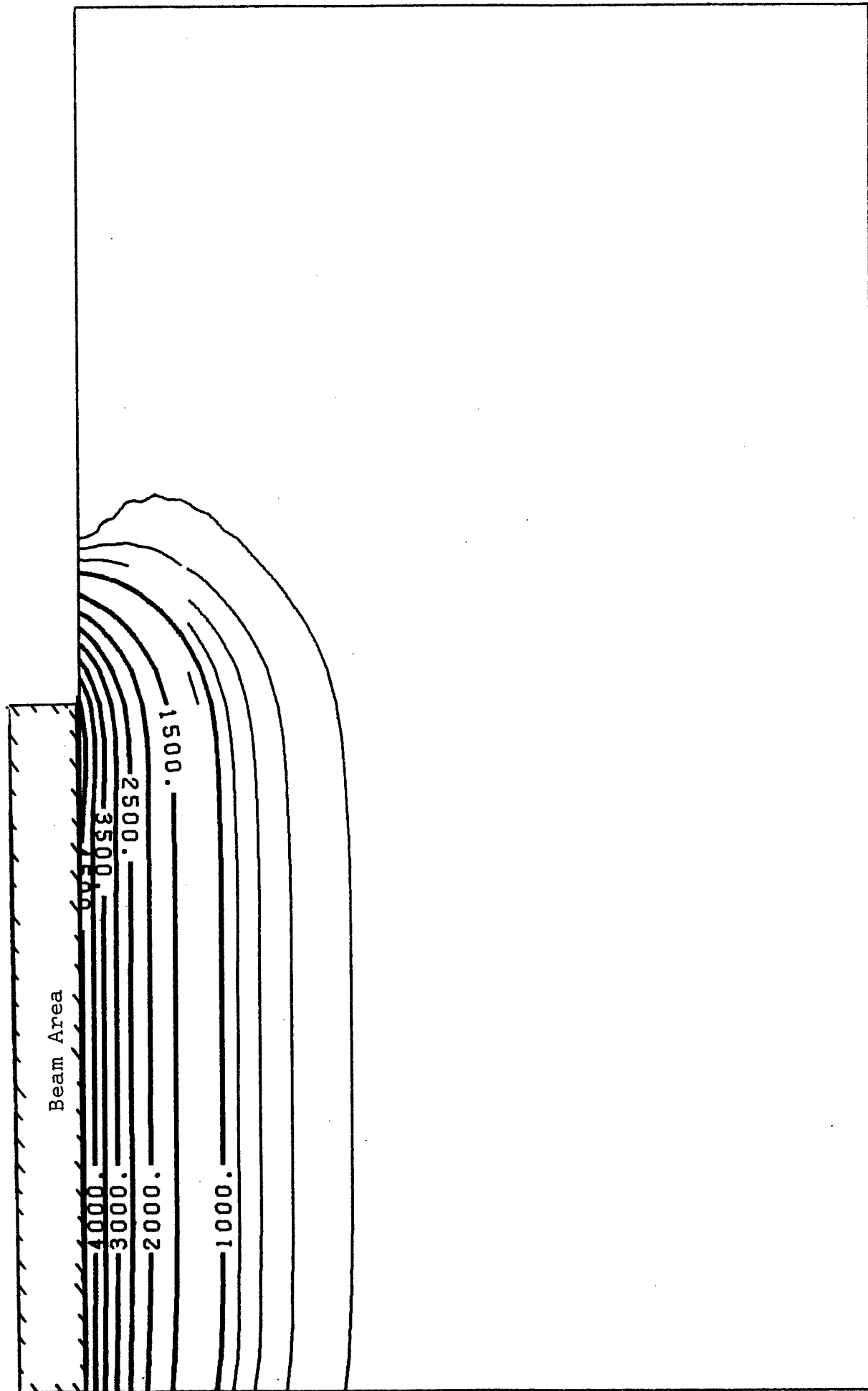


Figure 23. Temperature Distribution, DISC 3C, 0.06 sec.

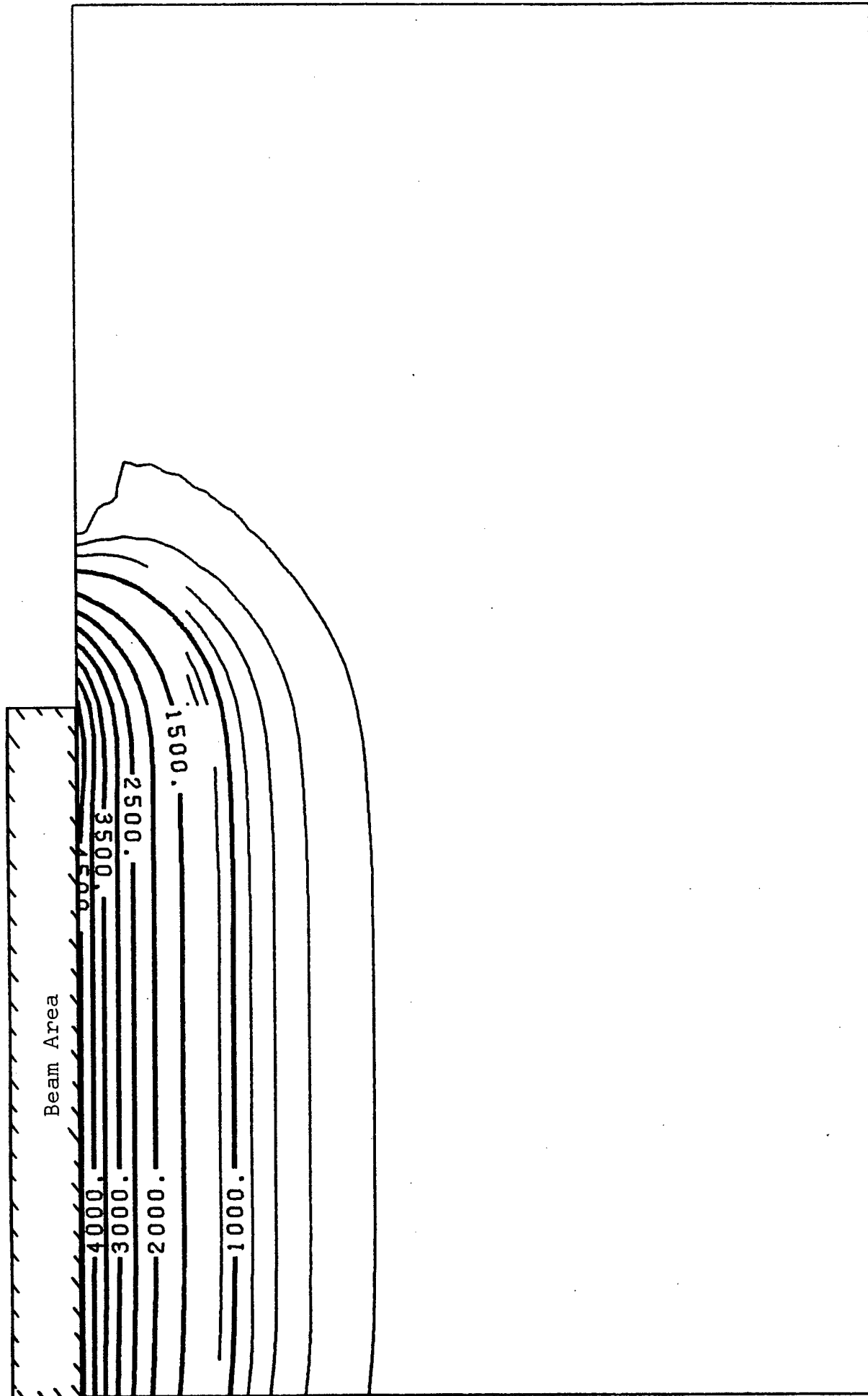


Figure 24. Temperature Distribution, DISC 3C, 0.07 sec.

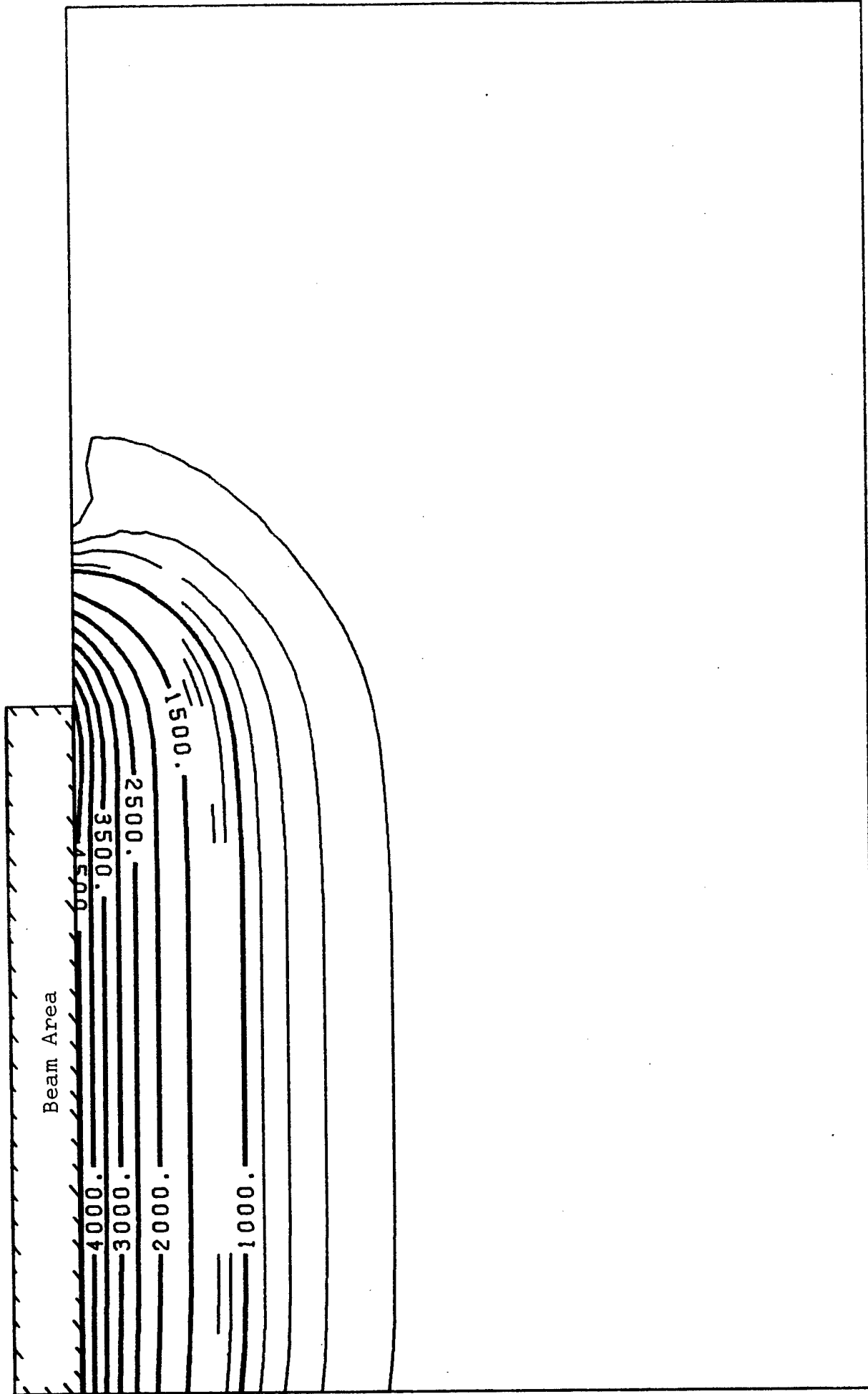


Figure 25. Temperature Distribution, DISC 3C, 0.08 sec.

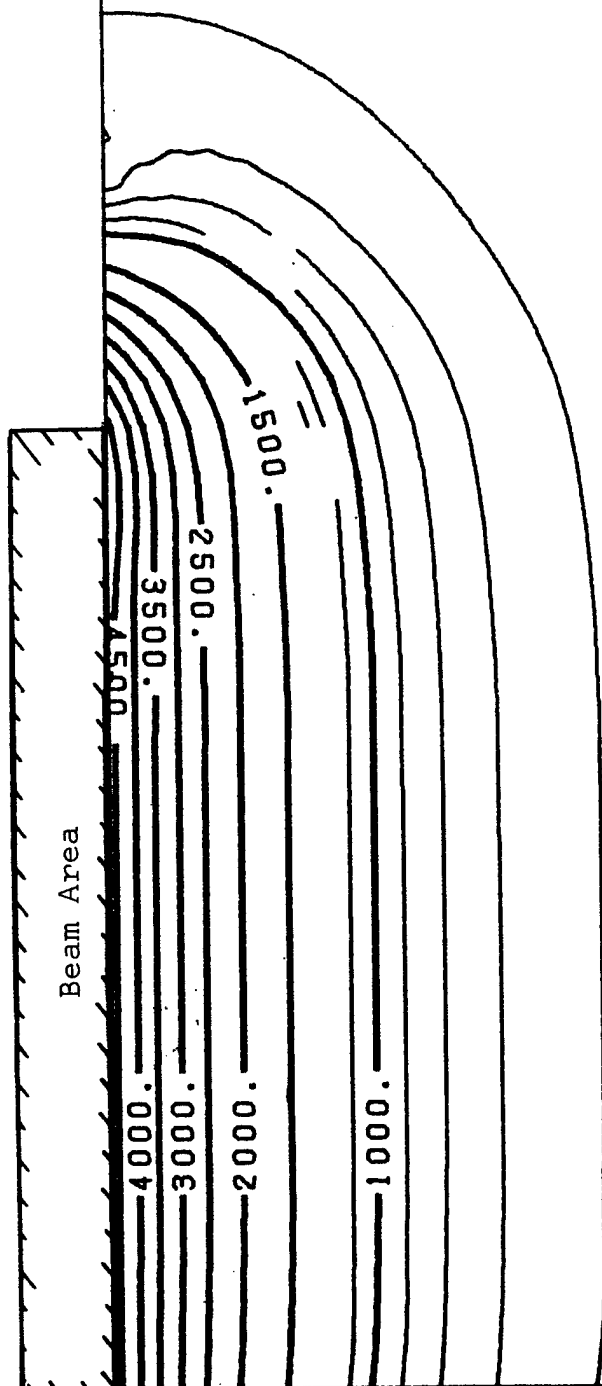


Figure 27. Temperature Distribution, DISC 3C, 0.10 sec.

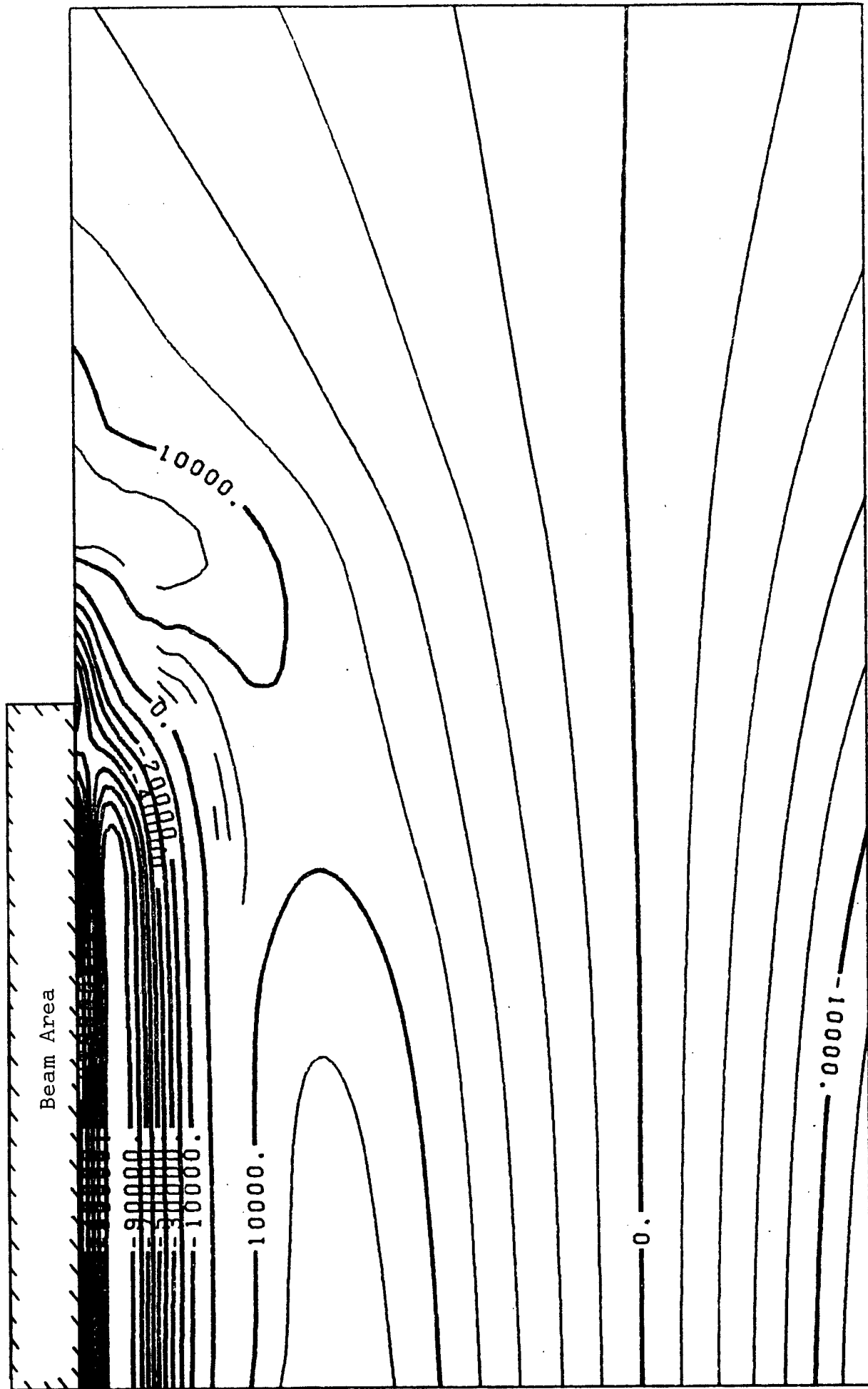


Figure 28. Hoop Stress Distribution, DISC 3C, 0.10 sec.

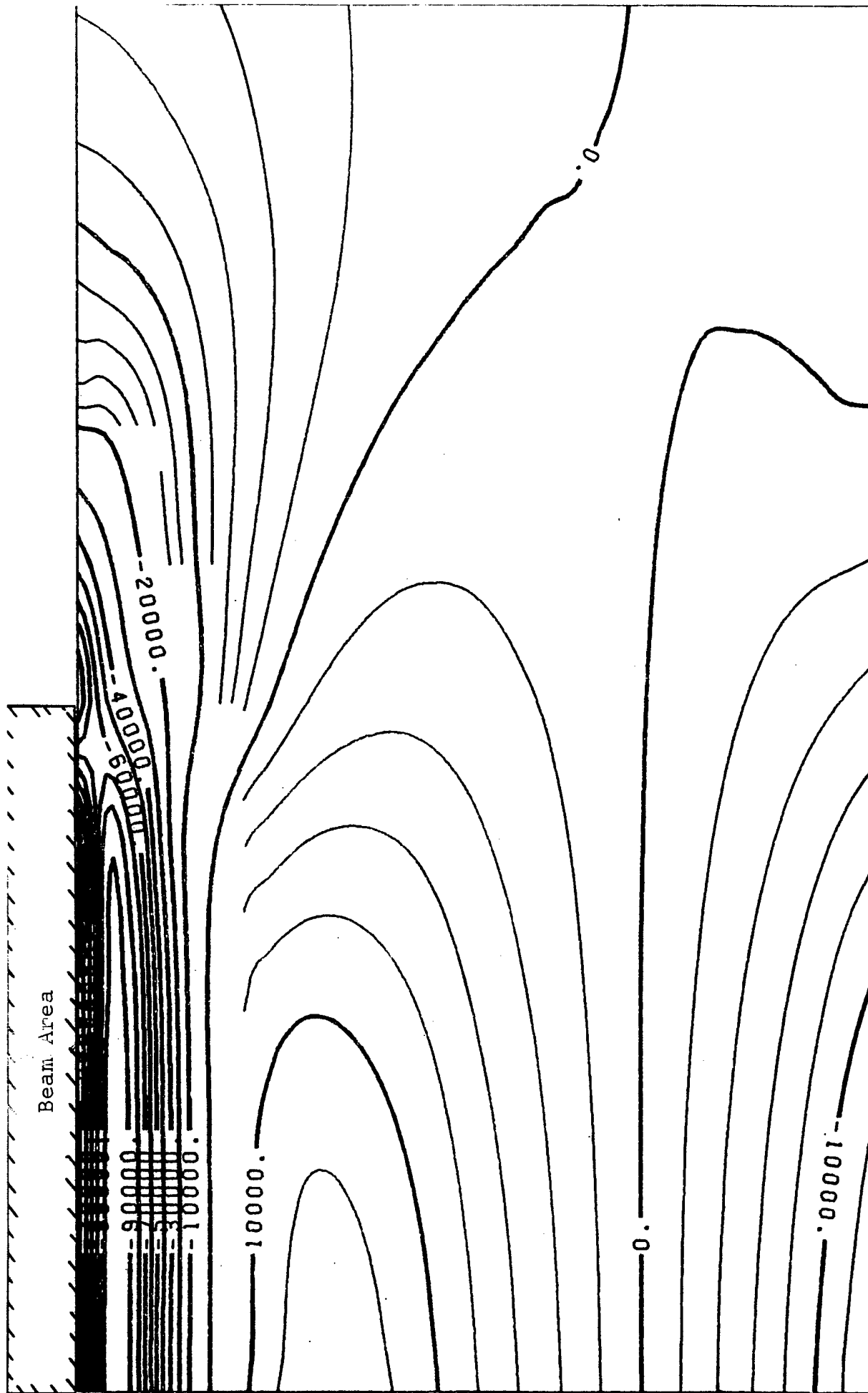


Figure 29. Radial Stress Distribution, DISC 3C, 0.10 sec.

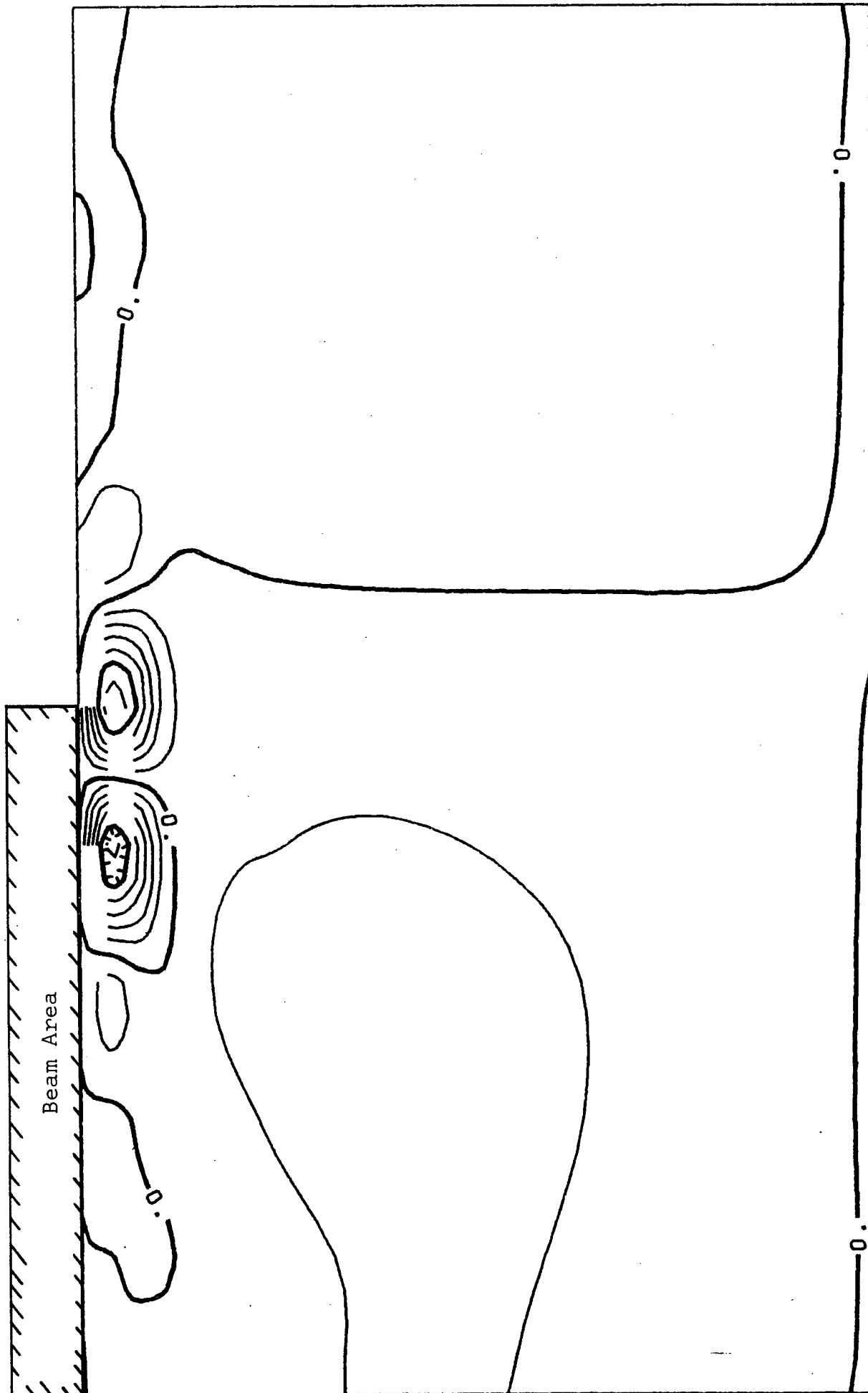


Figure 30. Axial Stress Distribution, DISC 3C, 0.10 sec.

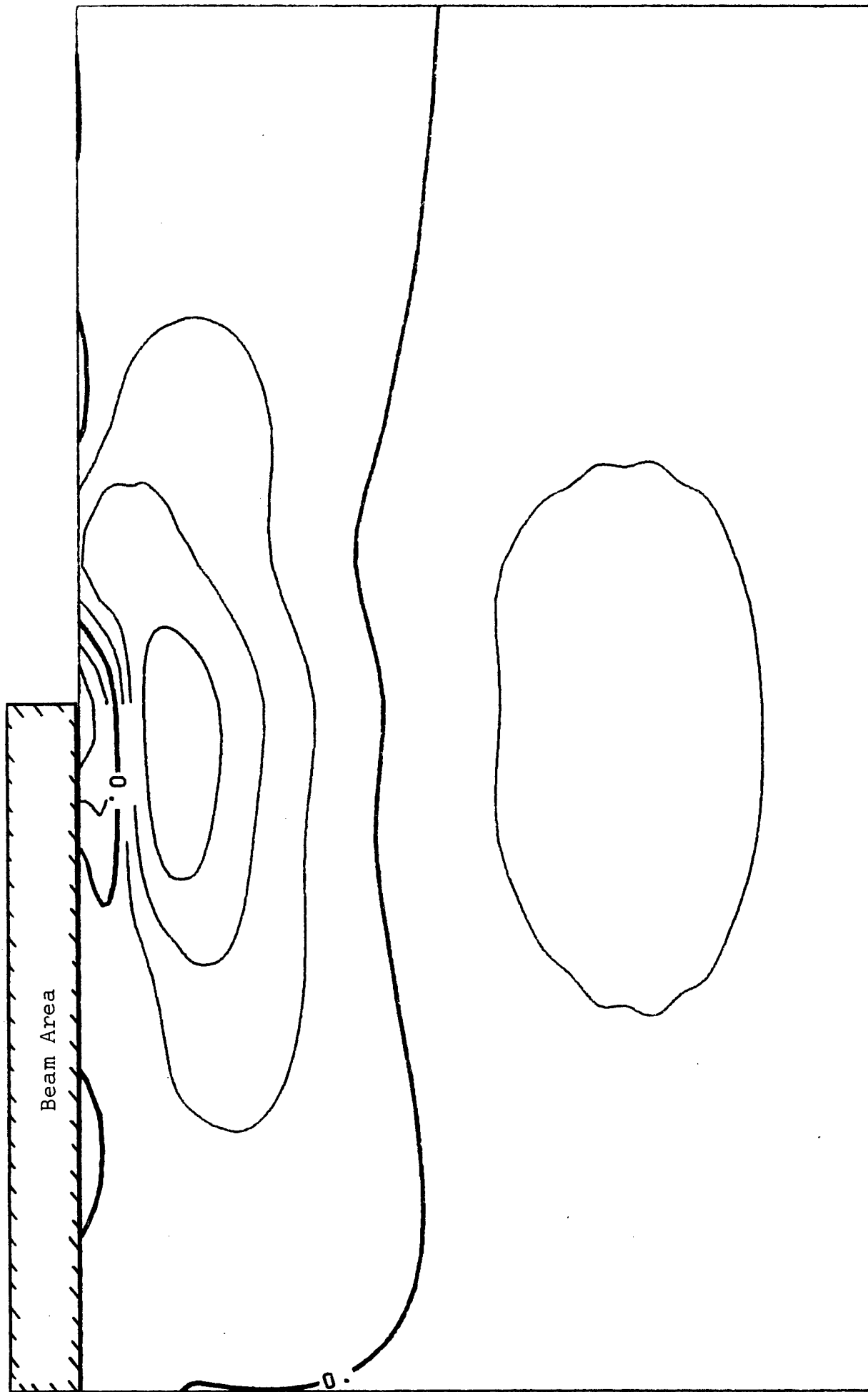


Figure 31. Shear Stress Distribution, DISC 3C, 0.10 sec.

seen to be considerably less than the width of the beam, so this assumption is considered to be valid near the center.

SECTION 4

RADOME ANALYSIS

The radome was modeled as a shell of revolution. Using symmetry, it was necessary to model only half of the radome, using the axis of the incoming laser beam and the axis of the radome as a plane of symmetry as shown in Figure 32. Only the front eight inches of the radome was modeled and the first 1/4 inch of the nose tip was eliminated. Preliminary runs indicated that there would be no significant stresses outside of this region for the thermal case being analyzed. The actual radome modeled is 19.0 inches long, restrained at the base where it attaches to the missile. The effect of truncating the model at eight inches and leaving the truncated end free is to neglect the bending moment which may occur here. The stresses obtained were therefore lower than would actually occur. On the other hand, clamping this end or otherwise restraining it would likely cause artificially high stresses since some radial displacement would actually occur here.

The element spacing is shown in Figure 32. Four 20 node isoparametric elements (CIHEX2) were used through the thickness of the radome. These had thicknesses of 0.02, 0.04, 0.10, and 0.10 inches starting at the outer surface. This meant that there were nine nodal points along the edge of each element with spacings of 0.01, 0.01, 0.02, 0.02, 0.05, 0.05, 0.05, and 0.05 inches, respectively. This grid spacing and element aspect ratios were determined from a free plate study using the same type elements (Ref. [4]). This corresponds to the DISC 1. spacing which was known to be marginal for the CTRAPRG elements. Ideally more elements were needed through the thickness in order to use the spacing determined to be necessary from the results of the DISC 3 study. However, this NASTRAN model was as large as could conveniently be run so this was not attempted. Adding more elements through the thickness or along the surface was

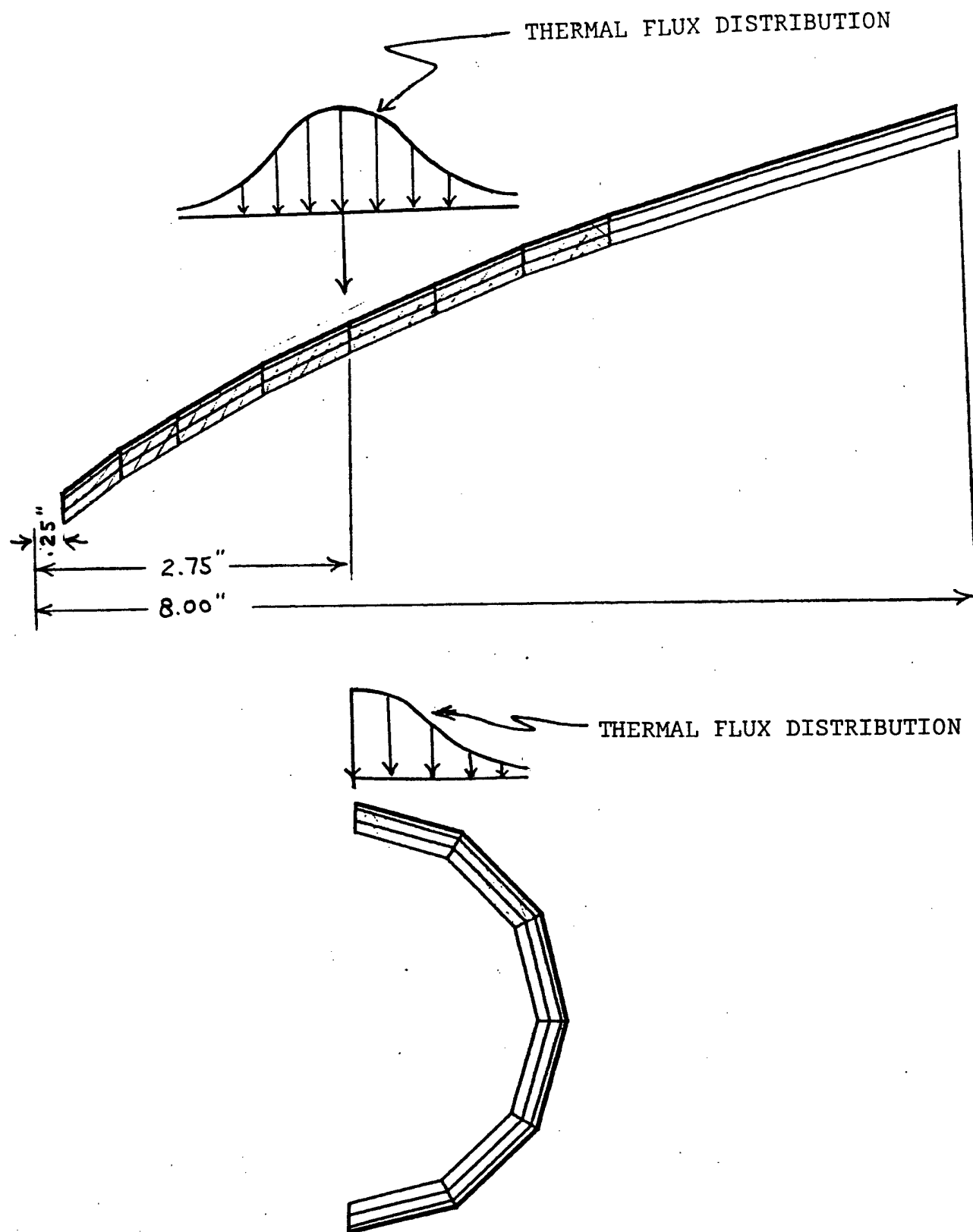


Figure 32. Axial and Radial Cross-Section of Radome Model

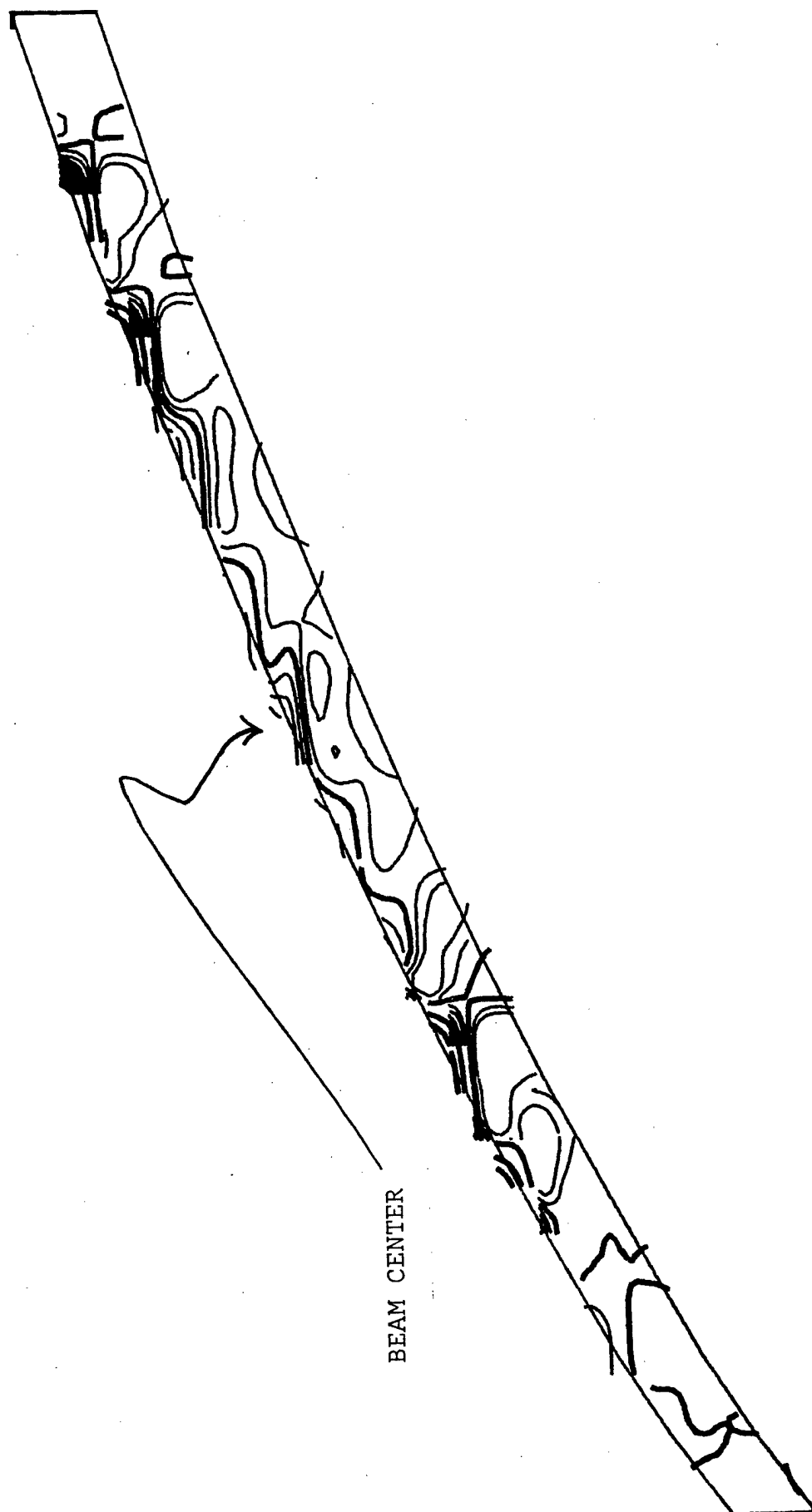
not considered feasible. The results of this decision can be seen later.

Grid point stresses were obtained from NASTRAN by saving the output and averaging the grid point stresses at all nodes, rather than using the element stresses. Results of the plate study (Ref. [4]) indicated that this provided a more continuous stress field and better results since nine data points were obtained through the thickness, rather than four if the average element stress was used. Results of the plate study also demonstrated that aspect ratios for the elements were not critical, provided that the only significant thermal gradient was in the thickness direction. Therefore, the aspect ratios used for the radome, although they appear to be high from Figure 32, are satisfactory in this regard.

The laser beam irradiation was simulated to occur at 2.75 inches from the nose tip and was perpendicular to the axis of the radome. A gaussian shaped beam with a one-sigma radius of 0.80 inches was simulated. An LTA model of the radome was constructed to obtain a three-dimensional temperature distribution for input to NASTRAN using the procedure outlined in Section 2. Since the flux was not constant on the surface as in the flat beam for the disc study, it was necessary to calculate the surface temperature at a number of flux levels using the 1-D program. The flux level at each external surface node within a two-sigma distance of the beam center was calculated for the LTA model as a function of the distance from the center and the exposed area due to radome curvature. These surface temperatures were then input to the LTA model to obtain the 3-D set of grid point temperatures needed for the NASTRAN input.

The results of the one-dimensional heat transfer program were also used in separate runs to determine if this was a reasonable alternative to conducting the 3-D LTA analysis. This was accomplished by calculating the flux level at each nodal location within a two-sigma radius of the beam center and

applying an adjusted one-dimensional temperature profile to the line of grid points through the thickness. The time steps used for both cases was 0.03 seconds. These results are compared in contour plots included as Figures 33 through 40. The sections shown in these plots are restricted to the shaded regions in Figure 32 since the stresses outside of this area were negligible. It can be seen from these figures that the shape of the stress distribution was somewhat the same but the values did not agree well. However, the mesh is too coarse to be able to create good contour plots. For a better comparison, axial, hoop, and normal stresses are compared through the thickness for the one-dimensional and three-dimensional temperature profiles. These data are fitted with a cubic spline fit as shown in Figures 41 through 46. Examination of these figures show that the three-dimensional temperature distribution predicts peak stresses approximately double that predicted from the one-dimensional temperature profile used as input to NASTRAN. This is a larger difference than one would expect from the disc study (Figure 6) where these stresses were only about 20 per cent higher. The peak hoop stress of 90,000 psi. compression from the three-dimensional temperature distribution (Figure 44) in the radome correlated most closely with the one-dimensional result of 85,000 psi. compression (Figure 6). This is approximately twice as high as predicted by Figure 43 where the 1-D temperature profiles were input to NASTRAN. However, analysis of these figures indicate the mesh size is too coarse to be sure that the peaks of these curves are obtained. The only firm conclusion that can be made from these plots is that the peak stresses obtained were almost identical to the one-dimensional AFFDL analysis.



BEAM CENTER

Figure 33. Hoop Stress Distribution Along Radome, 1-D Temperature

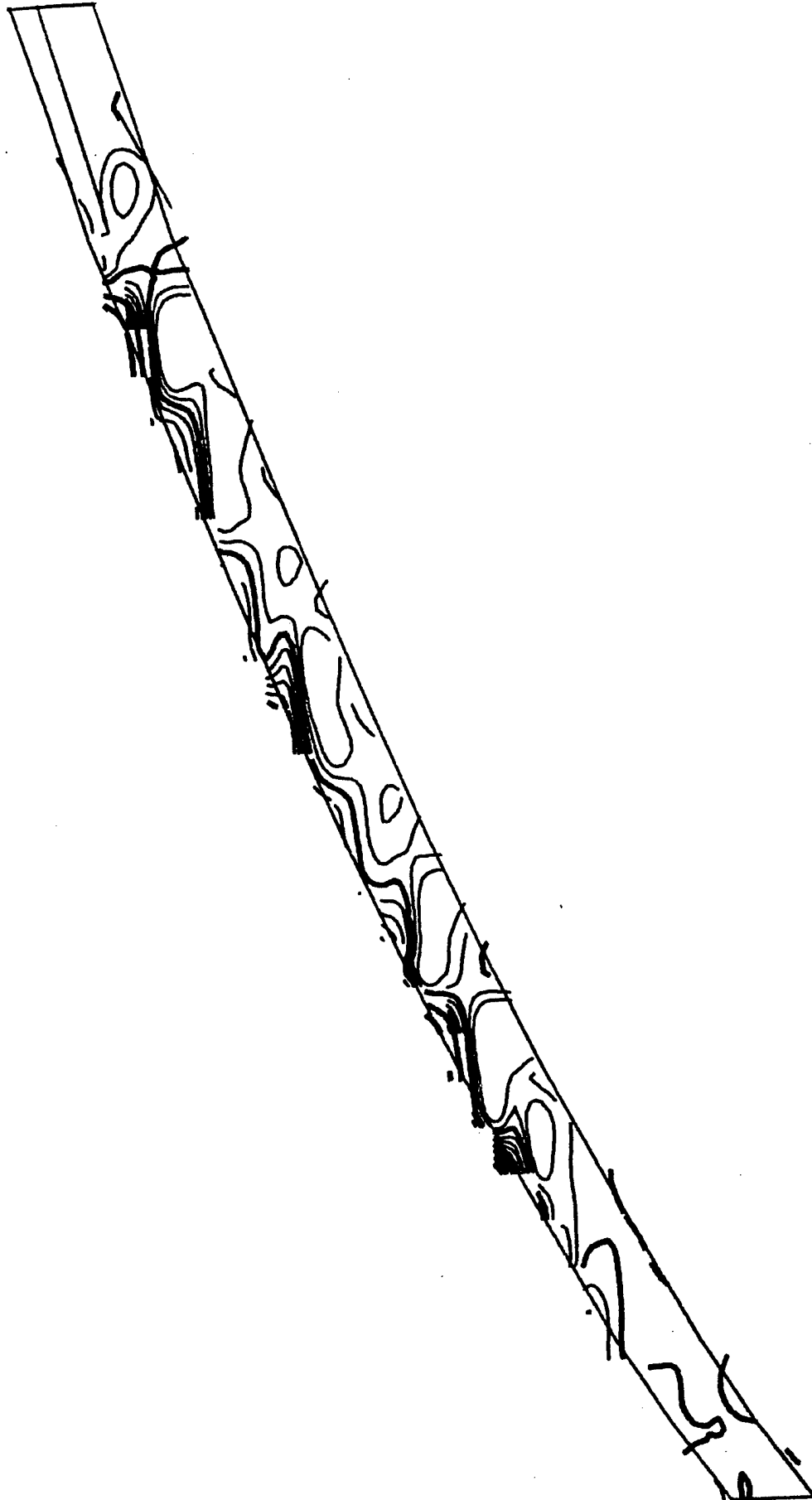


Figure 34. Hoop Stress Distribution Along Radome, 3-D Temperatures

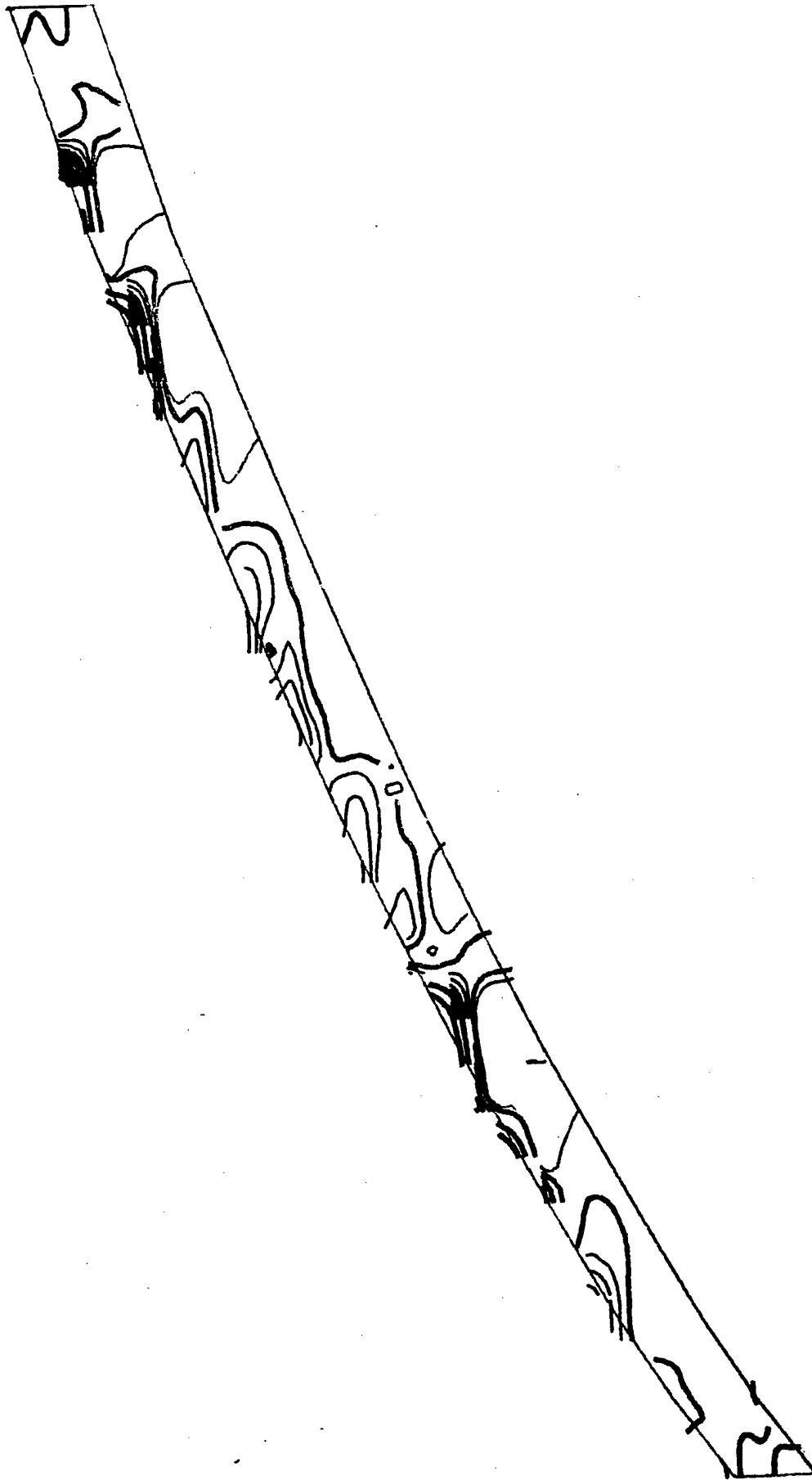


Figure 35. Axial Stress Distribution Along Radome, 1-D Temperature

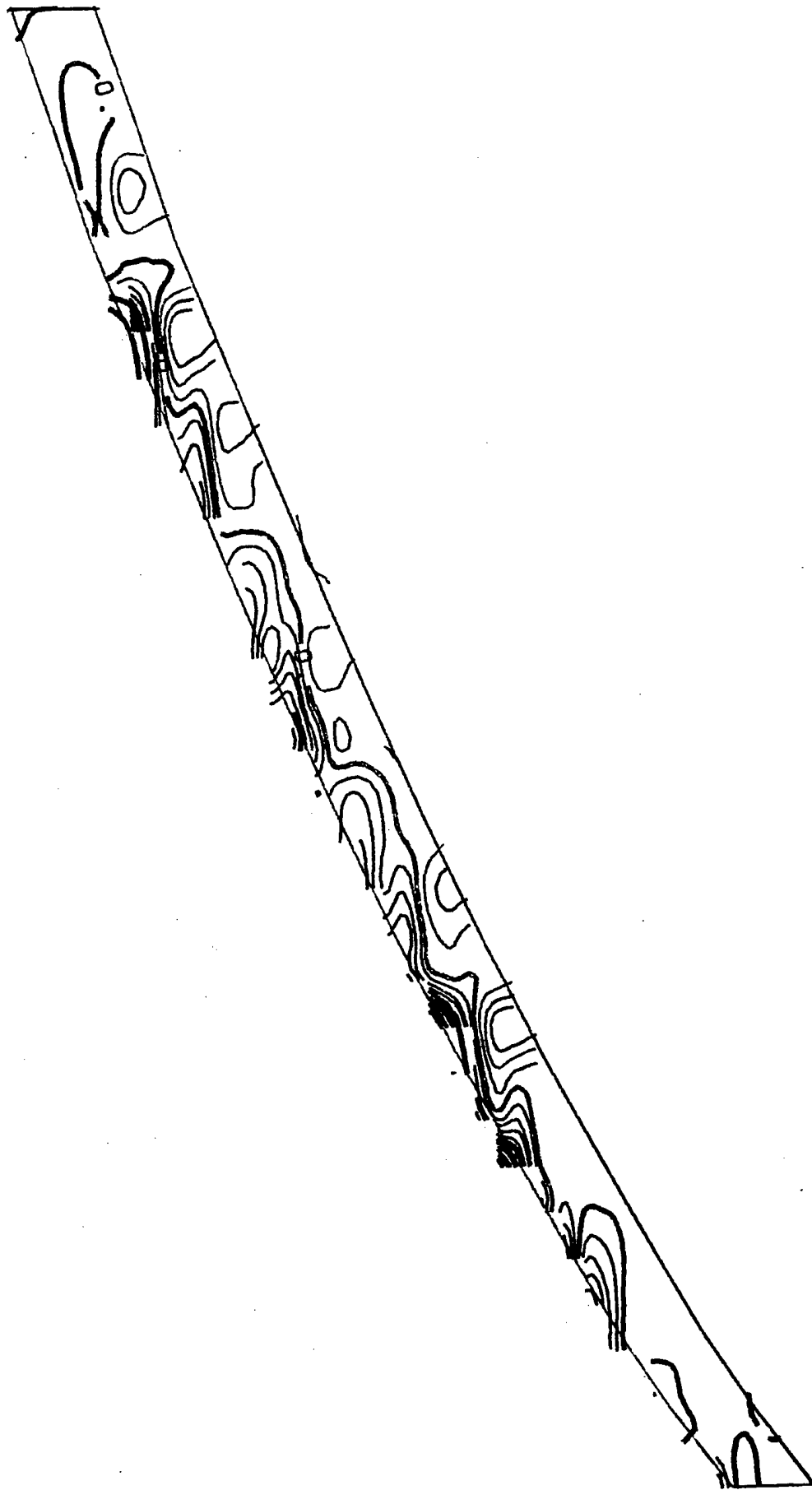


Figure 36. Axial Stress Distribution Along Radome, 3-D Temperature

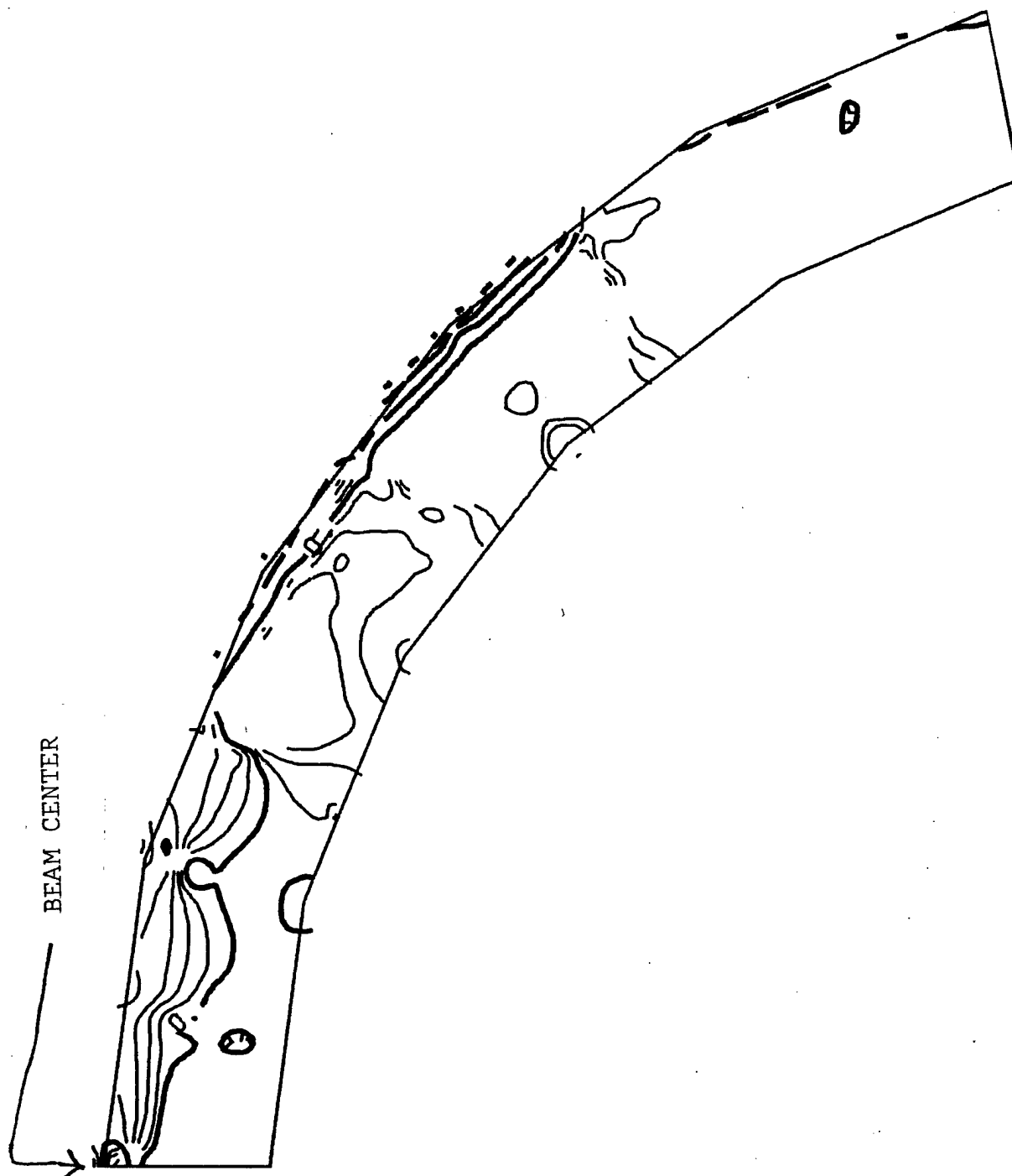


Figure 37. Axial Stress Distribution Across Radome, 1-D Temperature

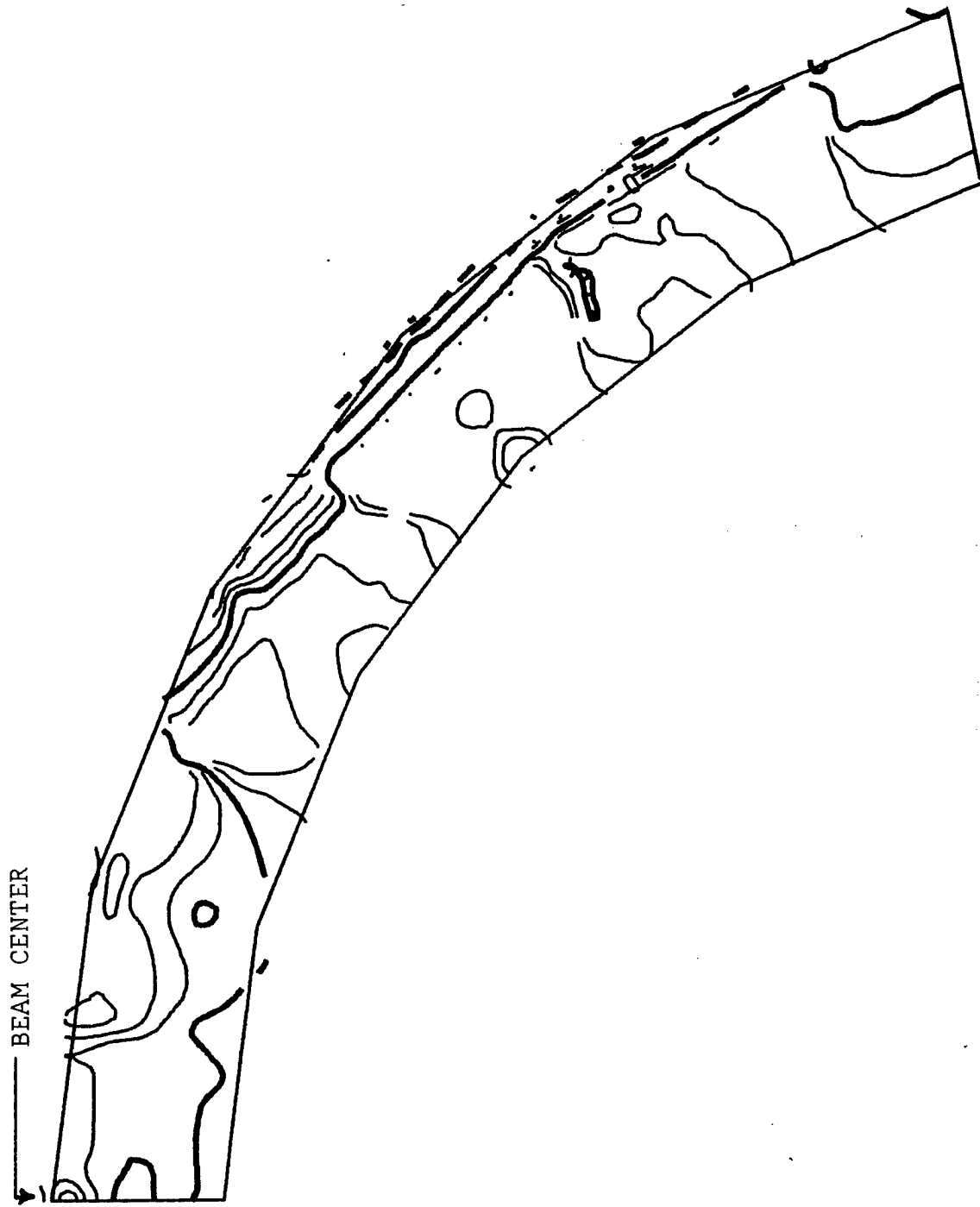


Figure 38. Axial Stress Distribution Across Radome, 3-D Temperature

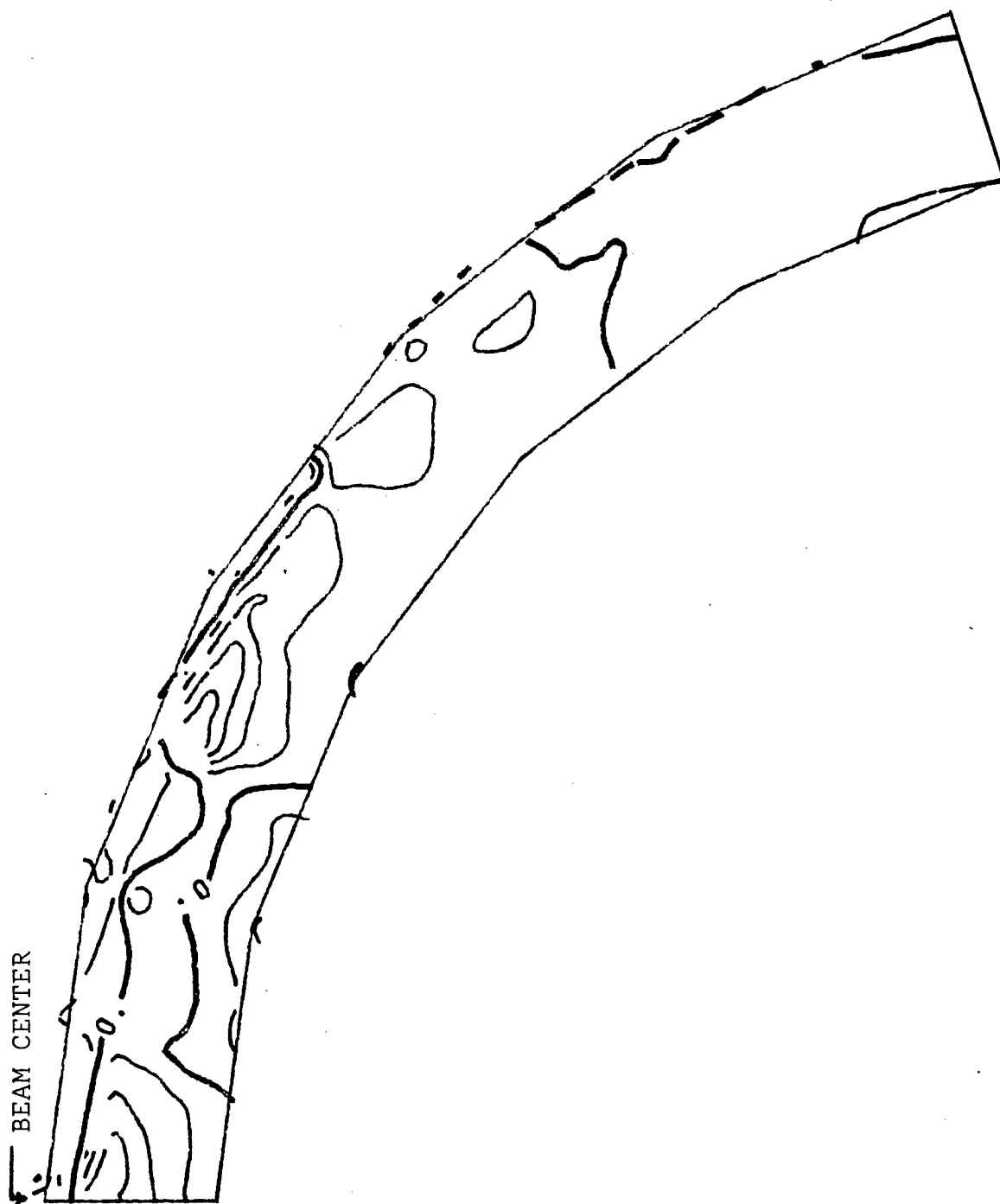


Figure 39. Hoop Stress Distribution Across Radome, 1-D Temperature

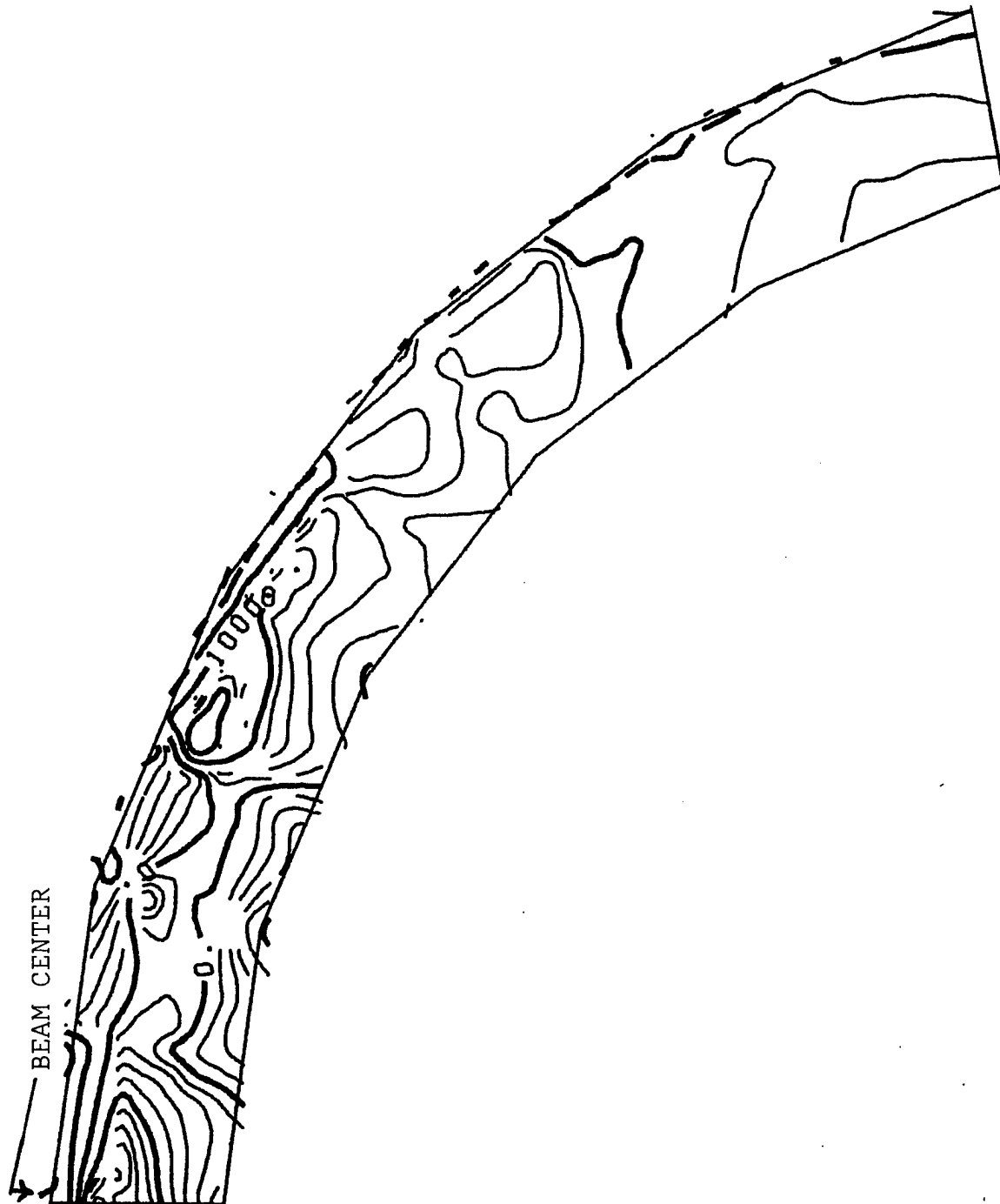


Figure 40. Hoop Stress Distribution Across Radome, 3-D Temperature

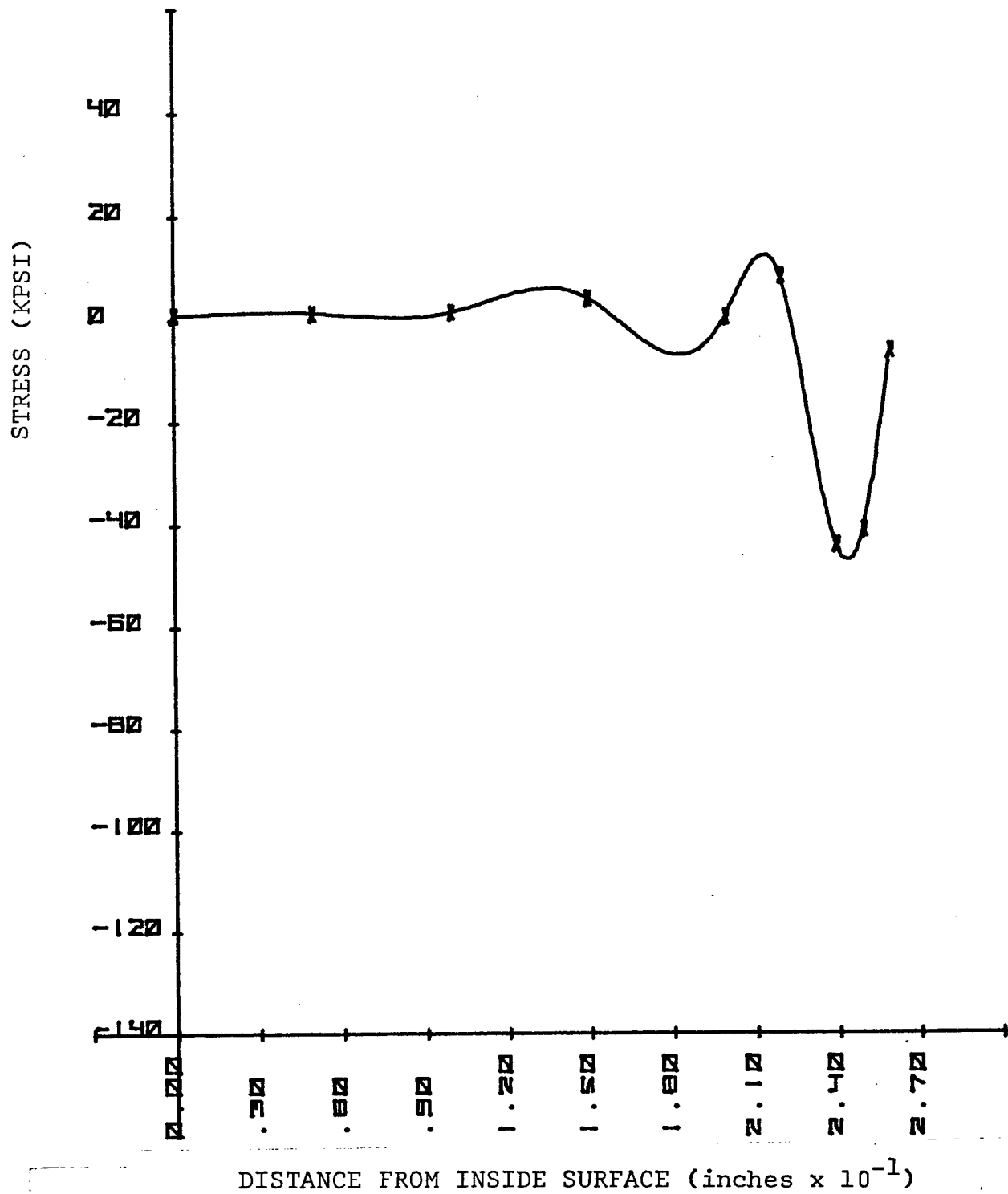


Figure 41. Axial Stress Distribution Through the Thickness at Beam Center, 1-D Temperature

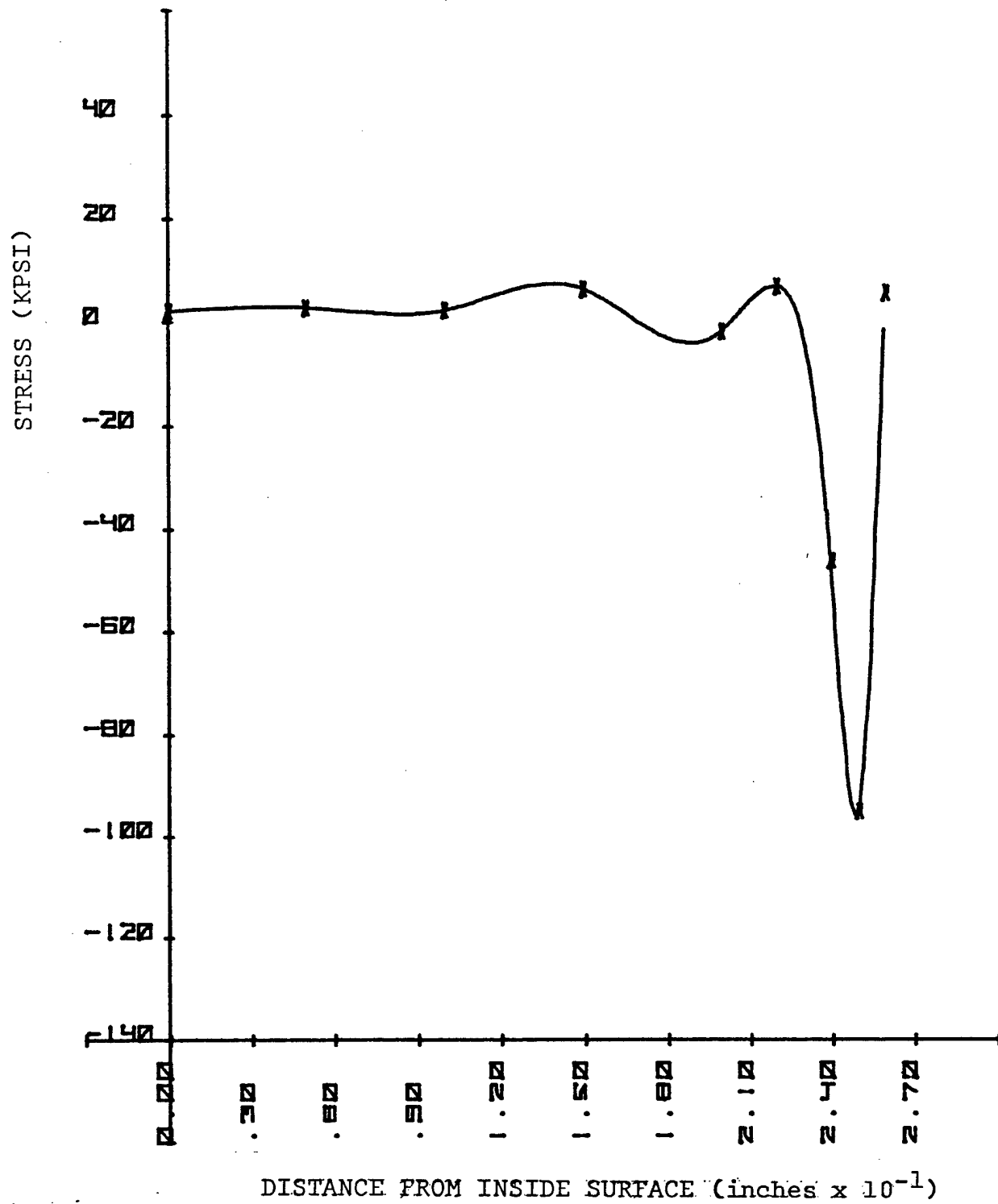


Figure 42. Axial Stress Distribution through the Thickness at Beam Center, 3-D Temperature

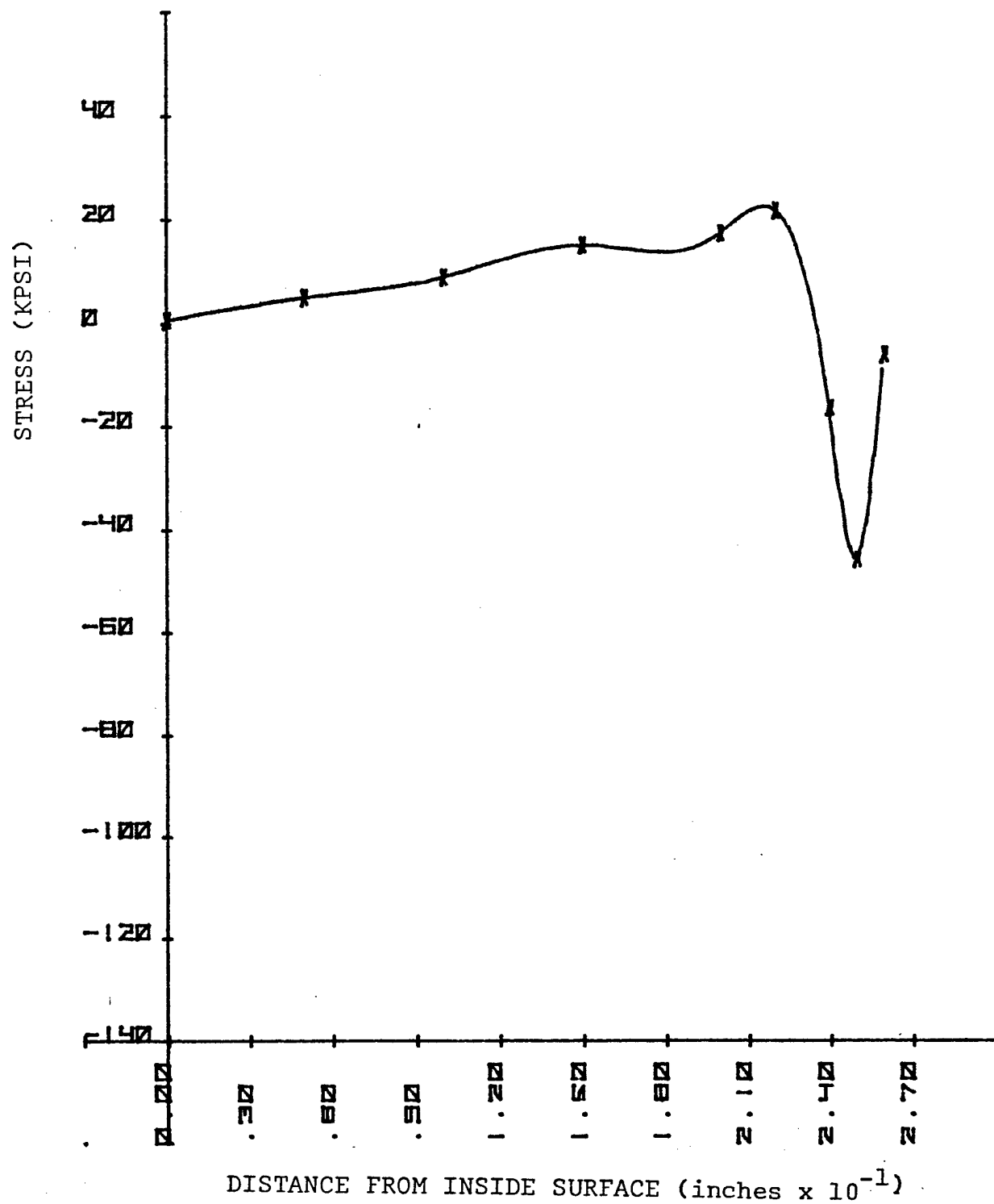


Figure 43. Hoop Stress Distribution Through the Thickness at Beam Center, 1-D Temperature

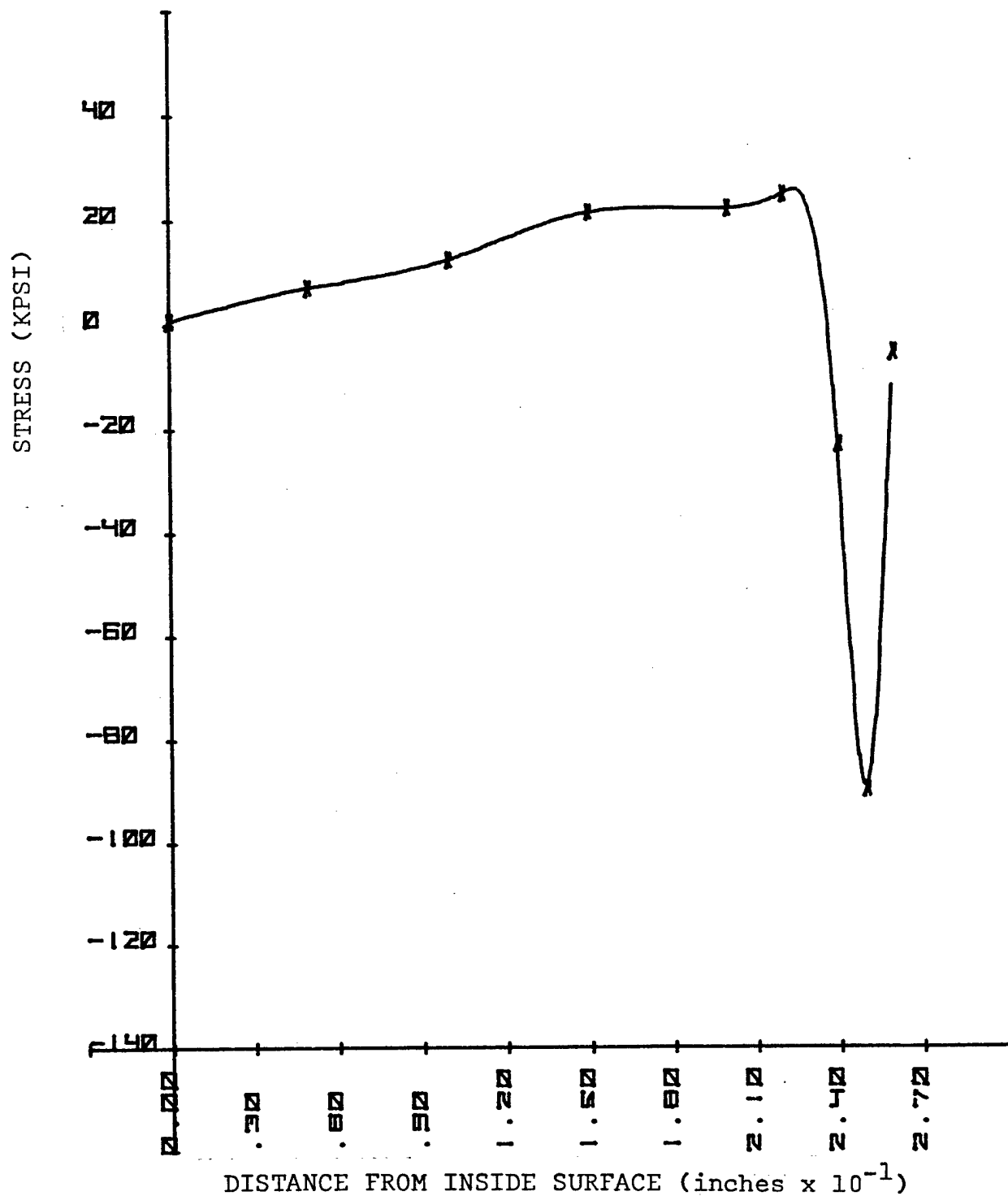


Figure 44. Hoop Stress Distribution Through the Thickness at Beam Center, 3-D Temperature

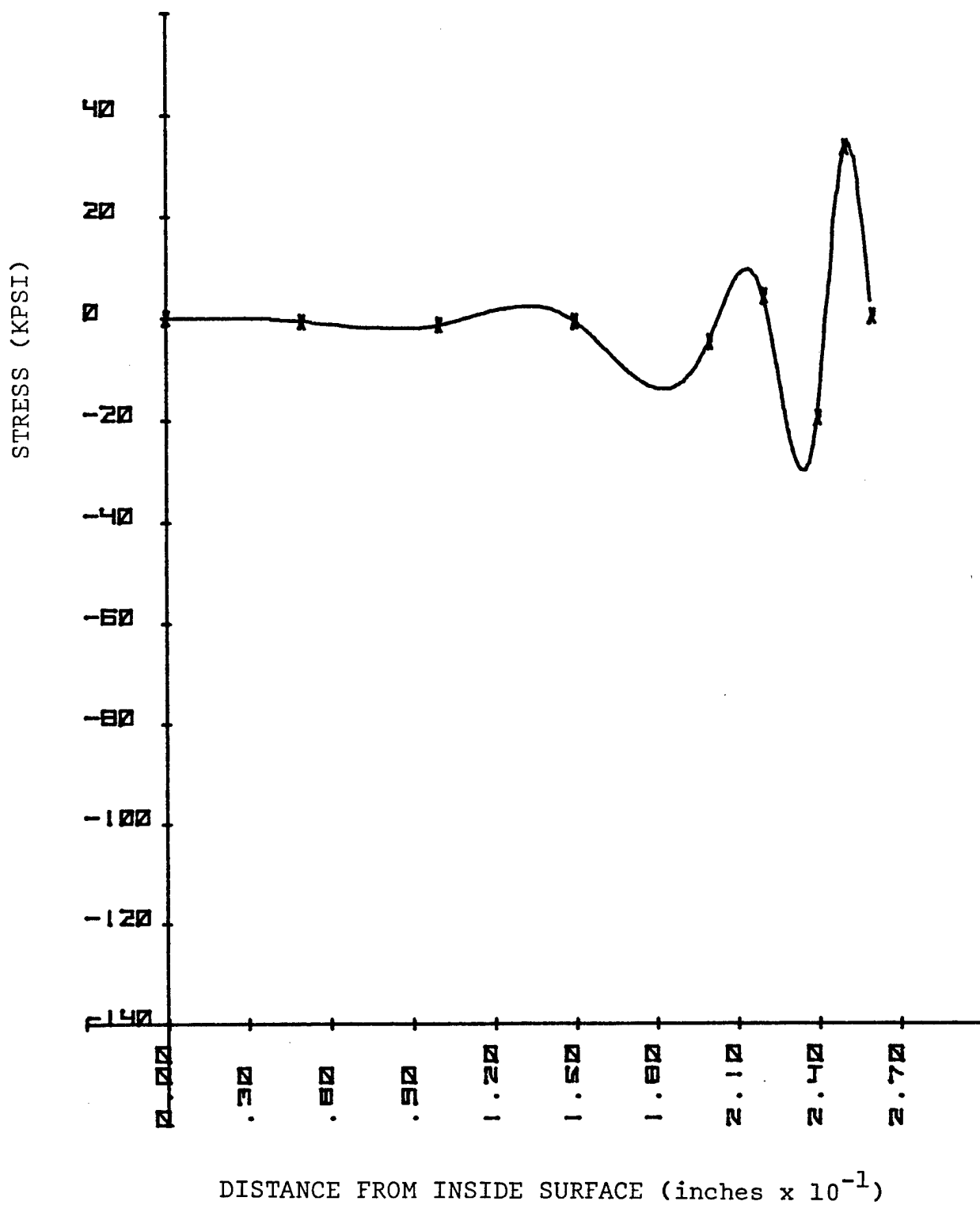


Figure 45. Normal Stress Distribution Through the Thickness at Beam Center, 1-D Temperature

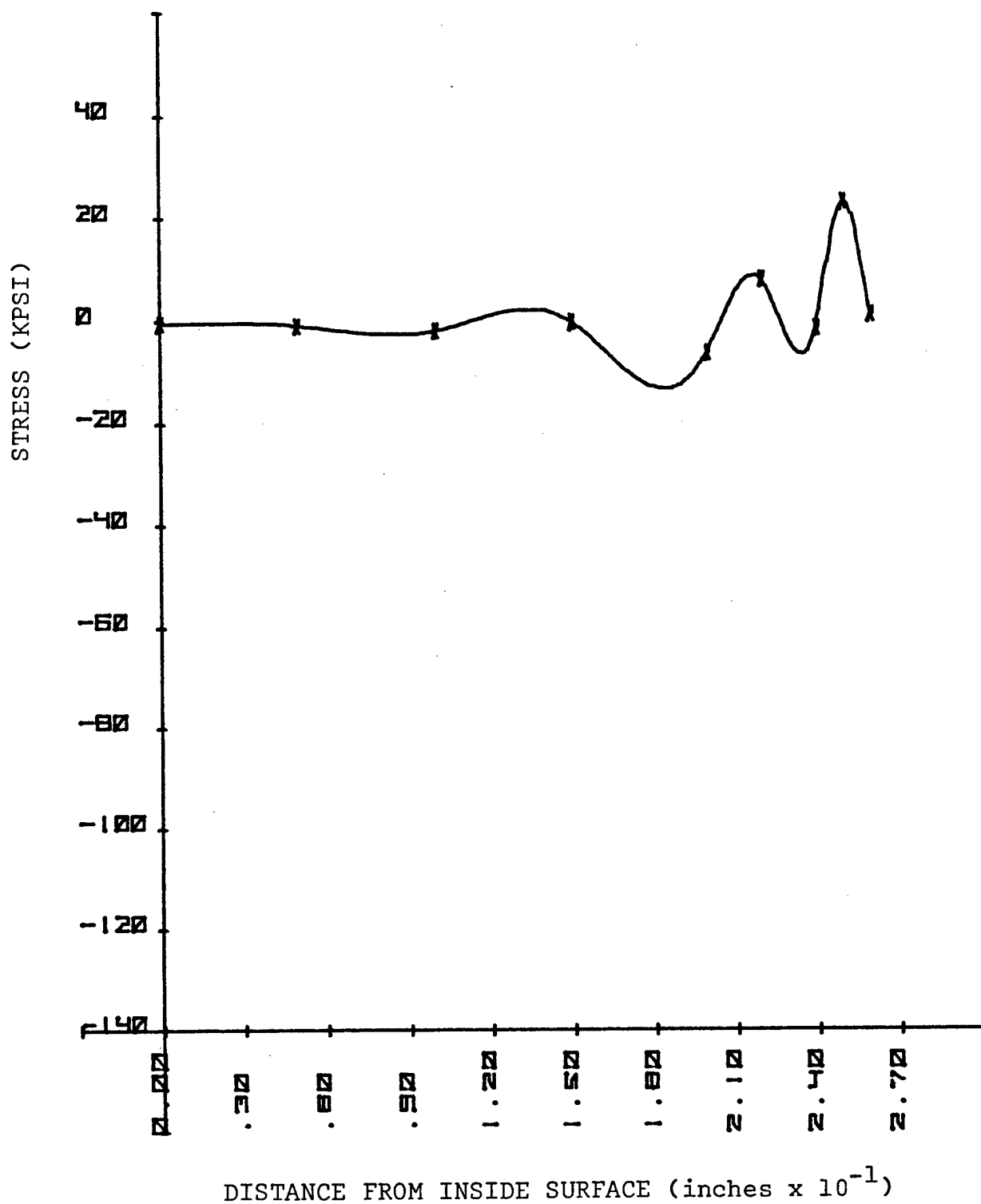


Figure 46. Normal Stress Distribution Through the Thickness at Beam Center, 3-D Temperature

SECTION 5

SUMMARY

The NASTRAN model of the radome used four layers of 20 node isoparametric solid elements (CIHEX2) with a total of 192 elements, 1118 grid points, and 3274 degrees of freedom. This model requires 240,000 octal words of central memory, 3690 CP seconds, and 2060 IO seconds for an adjusted computer cost of \$393.00 on the WPAFB CDC computer. By comparison, the much smaller, but finer disc model contained 899 axisymmetric elements (CTRAPRG), 930 grid points, and 1830 degrees of freedom. This model required 150,000 octal words of central memory, 790 CP seconds, and 530 IO seconds for an adjusted cost of \$70.00. As previously mentioned, LTA requires about 1000 CP seconds to calculate the temperatures for the radome, and 2000 CP seconds to perform the same calculations for the disc. By contrast, the AFFDL 1-D program required 52,000 octal words of central memory and 101 CP seconds for an adjusted cost of \$4.08 to predict essentially the same peak stresses.

The above statistics are presented to illustrate the difficulties involved, and should not be used to conclude that a three-dimensional thermal stress analysis cannot or should not be done. A 3-D analysis can reveal information about the pattern and interaction of the stress field that a 1-D analysis cannot do. Within the limitations of NASTRAN level 16.0 and the WPAFB CDC 6600, these were about the best results that could be produced. There were two techniques available for axisymmetric structures with asymmetric loading that were not tested in this study. The axisymmetric element (CTRAPAX) has this capability. The other technique is the use of solid elements using cyclic symmetry. Another possibility is the use of a next generation computer, such as the CDC 7600, with a much larger model.

The real limiting factor in this analysis was the number of nodal points for which LTA could provide temperatures. Other

thermal programs that have been examined also appear to be limited to about 1000 nodal points; however, it is possible that they could be increased in size more easily than LTA. A larger NASTRAN model is only feasible if a larger thermal program can be found. An alternative is to use the thermal analysis capability in NASTRAN itself. Sublimation or ablation would have to be ignored if this was to be done. The model would then be limited only by the NASTRAN-computer combination.

REFERENCES

1. Anon, "The NASTRAN User's Manual," Level 16.0, NASA SP-222(03), 1977.
2. Logan, C. C., David, R. B., and Michel, L. H., "Thermal Analyzer," Lockheed California Company, Report No. LR17708, March, 1964.
3. Paul, D. B., "Thermal Structural Analysis of Plates Subjected to High Energy Irradiation," AFFDL TR, to be published.
4. Lamberson, S. E., and Paul, D. B., "Thermal Stress Analysis of Ceramic Structures with NASTRAN Isoparametric Solid Elements," Seventh NASTRAN User's Colloquium, NASA CP-2062, October, 1978, pp. 207-215.